Journal of Analysis and Testing (2018) 2:26–44
https://doi.org/10.1007/s41664-018-0053-9

REVIEW

SERS Nanotags and Their Applications in Biosensing and Bioimaging

Wei Zhang[1,2] · Lianmei Jiang[2,3] · James A. Piper[2,3] · Yuling Wang[1,2]

Received: 23 December 2017 / Revised: 28 March 2018 / Accepted: 30 March 2018 / Published online: 23 April 2018

Abstract
Owing to the unique advantages of surface enhanced Raman scattering (SERS) in high sensitivity, specificity, multiplexing capability and photostability, it has been widely used in many applications, among which SERS biosensing and bioimaging are the focus in recent years. The successful applications of SERS for non-invasive biomarker detection and bioimaging under in vitro, in vivo and ex vivo conditions, offer significant clinical information to improve diagnostic and prognostic outcomes. This review provides recent developments and applications of SERS, in particular SERS nanotags in biosensing and bioimaging, describing case studies in which different types of biomarkers have been investigated, as well as outlining future challenges that need to be addressed before SERS sees both pathological and clinical use.

Keywords SERS · Plasmonic nanostructure · Nanotags · Biosensing · Bioimaging · Biomarker

1 Introduction

It has been known that Raman spectroscopy can provide rich structural, qualitative and quantitative information of analytes through their sharp and distinguishable vibrational bands of functional groups. Conventional Raman spectroscopy is not sensitive and in most cases requires a large integration time, potentially resulting in damage to the sample [1]. However, the situation changed since 1970s as enhanced Raman scattering of molecules was observed by using a roughened metal surface such as silver (Ag), which could enhance by several orders of magnitude for the Raman signal of an analyte located in its proximity [2–4]. Since then, scientists have made significant progress toward an adequate understanding of the fundamental concepts of surface enhanced Raman scattering (SERS). Typically, the enhancement mechanisms for SERS include chemical enhancement (CM) [5–7] and electromagnetic enhancement (EM), with the EM playing a predominant role [8–15]. While, the EM enhancement is the highest in a so-called "hot spot", which may be generated by excitation of a localized surface plasmon resonance (LSPR) in metal nanoparticles (NPs) with very close distances. The generated large EM field leads to a significantly increased sensitivity down to the single-molecule level [15–19]. Based on this concept, SERS-active substrates have usually been made to support plasmonic field and enhance the Raman signal with exquisite sensitivity. In regards to the application of SERS in biosensing and bioimaging, the unique advantages of SERS include: (i) the great multiplexing capacity for simultaneous detection and imaging of the targets, which is due to the narrow width of the vibrational Raman bands; (ii) quantification based on a specific SERS fingerprint of the corresponding molecules, conformation and structural studies of the targets; (iii) high photostability and optimal contrast with the red or near-infrared (NIR) excitation, which will minimize the fluorescence background, in particularly the autofluorescence from biological samples, such as blood, urine and tissue [20–22].

Biomarkers have been described as characteristics, most often molecular, that provide information about biological states, whether normal, pathological, or therapeutically modified. They have enormous potential to assist in the diagnosis, disease monitoring, and therapeutic effectiveness evaluation. Thus, non-invasive detection of the biomarkers in body fluids, such as blood, urine and saliva [23–25], holds great clinical potential for diagnosis and

✉ Yuling Wang
yuling.wang@mq.edu.au

1 Department of Molecular Sciences, Macquarie University, Sydney, NSW 2109, Australia

2 ARC Centre of Excellence for Nanoscale BioPhotonics (CNBP), Macquarie University, Sydney, NSW 2109, Australia

3 Department of Physics and Astronomy, Macquarie University, Sydney, NSW 2109, Australia

treatment monitoring. Furthermore, simultaneous detection of multiple biomarkers at very early stage provides an added value in improving the diagnostic accuracy. However, many biomarkers, such as those associated with cancer, have been identified in the concentration range of a few ng/ml, which is a big challenge for most analytical methods. For example, the typical detection methods for protein biomarkers are enzyme-linked immunoassay (ELISA), radioactive immunoassays, western blot, mass spectrometry (MS), or a combination thereof [26]. MS is highly sensitive but often needs to purify the protein samples before analysis [27]. Immunoassays are less time consuming, however, their sensitivity and quantitation abilities are inferior to MS and can only operate within a small range (from 1 ng to 1 μg/mL) [28]. More recently, SERS-based biomarker sensing has attracted much attention due to their versatile advantages in high sensitivity, excellent multiplexing ability, and wide working range. Two typical approaches, label-free SERS and SERS label, have been reported for biomarker detection. Label-free SERS is a directed and non-destructive approach to analyse and quantify the biomarkers with the limited specificity and intensive post-analysis due to the similarity of the vibrational peaks from the biomolecules. Whereas, SERS label is an indirect way to detect specific target through the probe and the ligand molecule on SERS nanotags. As a consequence, the number of research papers on SERS in biomedical applications has grown exponentially and has been summarized in excellent Review articles [29, 30]. SERS based methods are widely used in various biosensing, including pH, proteins, nucleic acids and many other biomarkers, developing a powerful sensing platform to fundamental research and real-world applications [26, 30]. Moreover, SERS is also increasingly used for bioimaging [31, 32]. SERS-based bioimaging shows great potential to make SERS an important diagnostic tool to complement other imaging techniques, such as magnetic resonance imaging (MRI), fluorescence imaging and computed tomography, owing to its single cell sensitivity that diagnostic counterparts of many methods lack [33]. More importantly, SERS bioimaging can support a pathologist with adequate clinic related information under in vitro, in vivo and ex vivo conditions, providing the decisive advantage with information which can be directly obtained from the samples (e.g., cells, tissues). Therefore, SERS has the potential to become a primary imaging tool for early disease detection or post-operative outcome monitoring.

In this review, we summarize the recent advances of SERS nanotags for biosensing and bioimaging. The review is structured as follows. First, a basic review of SERS NPs and SERS nanotags are discussed. Then a detailed summary of SERS application in detection of various types of biomarkers is presented, along with the development of SERS bioimaging in biomedical field. Finally, we give an outlook on the future challenges of SERS in biosensing and bioimaging.

2 SERS Nanoparticles

2.1 Plasmonic Nanostructures

The success of SERS applications mainly depends on the interaction between adsorbed molecules and the metal surface, which is a rapidly emerging research area known as plasmonic nanostructure. Classic plasmonic nanostructures such as gold (Au), Ag, and copper (Cu) have the common optical property that their LSPRs cover most of the visible and near infrared wavelength range, where most Raman measurements occur. [34]. In general, Au is the most broadly used metal because of its easily controlled sizes, good stability and outstanding biocompatibility [35]. Ag usually exhibits the highest SERS signal in the visible region [36]. On the other hand, Au shows a strong excitation close to the IR region of light and attracts considerable interests in the medical field compared to other metals [37, 38]. Apart from those mentioned-metals, alkali metals (Li, Na,etc.), Al, Ga, In, Pt, Rh, and metallic alloys [39] have also been explored as SERS substrate. Other materials including graphene [40], semiconductors such as TiO_2 [41], and quantum dots [42] have recently been reported to show SERS activity [34].

The plasmonic properties of metallic nanostructures include the resonance frequency of the localized surface plasmons (LSPs) and magnitude of the EM field generated at the surface [43]. These plasmonic properties can be tuned by changing the physical properties such as shape [44–47], size [48–51] and dimensionality (2D and 3D) [52–54] of the plasmonic nanostructures. Over the last 3 decades, researchers have made great progress in the development of SERS plasmonic nanostructures to maximize enhancement factors (EFs). Initially, plasmonic nanostructures were used basing on spherical NPs [55]. However, the position of the LSPR of spherical AuNPs shifts to respond the increase of plasmonic nanostructure size with a limited red shifts of ~100 nm at most [56]. As a result, spherical plasmonic nanostructures may not be the most suitable materials to be used for optimizing the EFs, owing to a limited overlap between the laser excitation frequency and the LSPR band [31]. Non-spherical plasmonic nanostructures have the advantage of possessing built-in hot spots [31]. Unlike nanospheres, nanorods have two plasmon resonance bands: the weaker transverse one in the visible range and the stronger longitudinal one in the longer wavelength range. The longitudinal one can be tuned from the visible to the NIR region by increasing the long axe of the nanorods, which permits for markedly improved laser penetration depth of tissue and is expected

for in vivo biosensing and bioimaging [30]. Similar isolated non-spherical plasmonic nanostructures, such as nanocages [57], nanostars [58], nanobars [59] and nanorice [60], are also widely proposed for SERS application, as they carry intrinsic hot spots. Various research groups have studied and reported the relationship between the enhancement and the shape/size of immobilized AuNPs using different analytes [61, 62].The results indicate that SERS enhancement is highly dependent on factors such as the geometry (e.g. size, shape) of NPs. The dimensionality of the plasmonic nanostructures is another factor that can affect the plasmonic properties. For example, 2D and 3D plasmonic nanostructures, especially 3D plasmonic nanostructures, have been successfully fabricated and used in SERS studies [63, 64]. Nowadays, with the advancement of nanotechnology, it is believed that more and more NPs could be fabricated with well-defined geometry for reproducible and uniform SERS signal generation.

2.2 SERS Nanotags

Dyes and molecule fluorophores are widely used labelling agents for specific detection of biomolecules. SERS nanotags, as an alternative label, provide unique optical properties and potential for simultaneous and multiple detection due to the advantages of SERS nanotags over the fluorescent labels including the multiplexing capability for simultaneous target detection, quantification using the SERS fingerprint and the need for only a single laser excitation wavelength, and high photostability [21, 22]. Typically, SERS nanotags (as shown in Fig. 1) include a metal colloid for Raman signal enhancement, Raman labels/reporter linked on the metal surface for identification, a protective layer or shell for NP stabilization, and a ligand (e.g. an antibody) for recognising the target [26, 65]. We will discuss briefly the chemical component and structure of SERS nanotags in this review.

Besides the metal colloids as discussed above, the choice of Ra molecules is also essential. Ideal Ra molecules should have the following advantages: (i) high Raman scattering cross sections for high signal levels such as dyes (Fig. 1a), (ii) a few atoms and/or high symmetry, resulting in a minimal number of Raman bands for multiplexing (Fig. 1b), (iii) low or no photobleaching for the stability of signal, and (iv) surface groups for binding the metal colloid surface with target molecules [22]. As an typical example, Graham et al. reported the use of either custom-built benzotriazoles [67] or commercially available dyes (BODIPY, Cy5.5, etc.) for multiplexed detection of DNA [68–70].

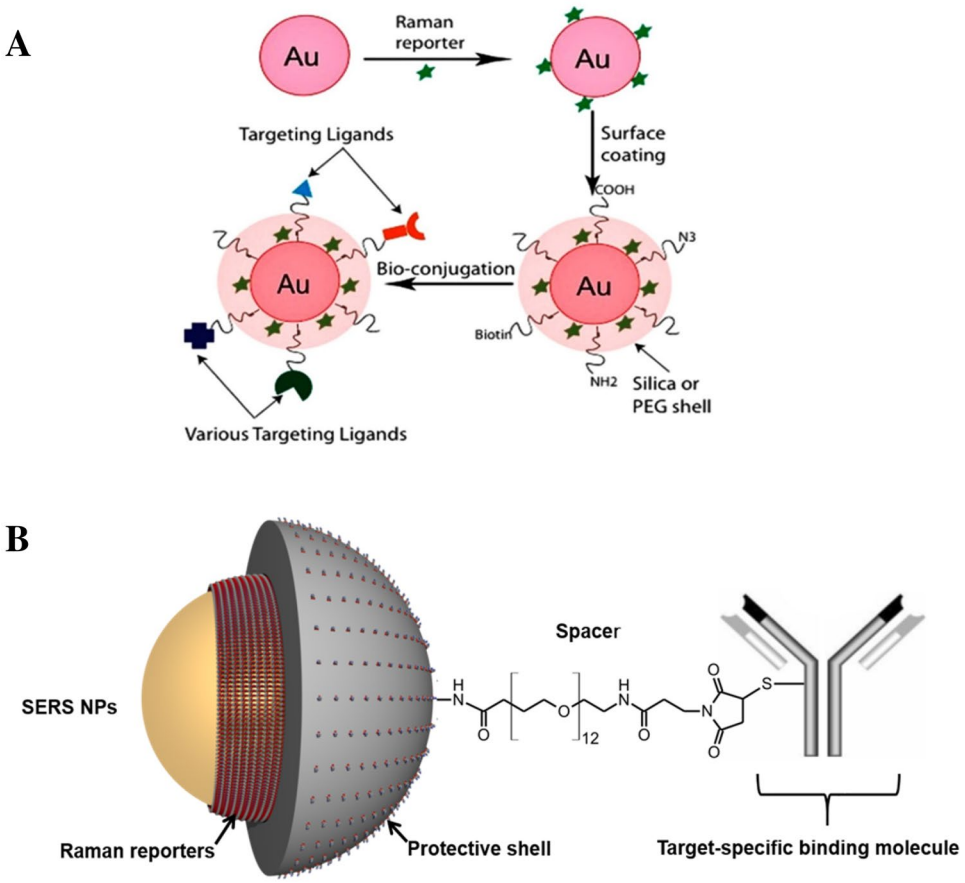

Fig. 1 Typical SERS nanotags, consisting of a metal nanoparticle core, Raman reporter (Ra) molecules (dye as Ra in A and self-assembly monolayer of small molecule as Ra in B) on the metal surface, a biocompatible layer, and targeting ligands. Cited from Ref. [26] and [66]

Protection and stabilization of SERS nanotags is important for practical use. Surface coating of SERS NPs is a way to stabilize the NPs against coalescence in physiological conditions [31]. Currently, three kinds of surface coating methods are commonly used: (i) biomolecules, such as bovine serum albumin (BSA), (ii) polymers, such as PEG, (iii) glasses, such as silica [33]. BSA is one of the most popular materials for SERS nanotag surface coating, owing to its well-known properties, e.g. biocompatibility and easy link with the NPs [30, 31]. Biocompatible polymeric coating, such as PEG, can increase the nanotag stability with retained biocompatibility, in the meantime, providing nanotag with chemical end groups that can be used for surface functionalization, which is important for binding targeting molecules on the nanotags [71]. Encapsulating the Raman reporter molecules and NP in silica shell is another option to protect and stabilize SERS nanotags [72, 73]. It is reported that SERS NPs having silica shells are stable in various chemical environments [73].

To recognize target molecules, SERS nanotags need to be conjugated to specific ligands, such as antibodies, depending on the specific cases. As discussed, SERS can work in direct and indirect detections for biomarkers [74]. Direct or label free SERS is highly powerful for the identification of analytes with rich aromatic rings and unsaturated bonds, but exhibit weak signals for analytes that do not have these groups [33]. Direct SERS detection is seldom used in medical field because of issues of opsonisation [33], while using SERS nanotags is more appropriate for the extremely heterogeneous environments in the medical field. In this approach, the target is recognized employing the targeting moieties bound to the NPs. The applications of this method are depicted substantially in sections of biosensing and bioimaging, and will not discuss here.

Furthermore, ideal SERS nanotags for biosensing and bioimaging applications should offer a high signal enhancement, induce a reproducible and uniform response, have a stable half-life and should be easy to synthesize [74–76]. Relevant studies have been reported. For instance, Lim and co-workers developed a DNA-AuNPs-based approach to prepare Au-NNPs, which have a well-defined 1 nm bridged hollow interior nanogap, with a high yield of 95%. The results indicated that the Au-NNPs SERS signals were highly strong, extremely quantitative and controllable depending on different factors [77]. This method further provides a synthetic platform to generate a new class of highly tailorable nanoprobes which can be used to deal with problems of low cross-section, signal reproducibility, quantification and sensitivity in solution-dispersed SERS nanotags. Additionally, Liu et al. reported a new type of SERS nanotags with hybrid multilayered nanoshells obtained by the layer-by-layer (LBL) assembly of small AgNPs at the surface of SiO_2 particles using poly(ethyleneimine) (PEI) [78]. The plasmonic coupling of AgNPs can enhance tremendous electromagnetic field, which makes SERS signal been detectable on a single particle level with highly narrow distribution of enhancement. Moreover, the cross-linkage of the hybrid shells can effectively avoid the leakage and oxidation of tag molecules. Therefore, the generated SERS signals are extremely uniform, reproducible, quantitative and stable. More recently, Cao et al. developed a SERS nanotag with a chemically-etched tapered fiber tip and silanized fiber taper [79]. They chose 4-aminothiophenol (4-ATP) as the target analyte to study the SERS responses of the obtained SERS nanotag in an optrode remote detection mode. The results indicated that the prepared SERS nanotags presented the ability to detect the 4-ATP molecule at a concentration as low as 10^{-9} M. This method also showed good reproducibility with the relative standard deviation (RSD) values being less than 9.1% for the strongest Raman peak. This study offers a novel and reliable way to obtain fiber SERS nanotags with high sensitivity, long-term stability, good reproducibility, and superior recyclability, holding great potential in SERS-based application.

3 Sensor Platform

Owing to the unique advantages of SERS nanotags, it offers an excellent platform for biosensing. Here, we will discuss the recent works on SERS biosensing applications, ranging from pH, proteins, nucleic acids and other disease relevant biomarkers as summarized in Table 1. Then we will emphasize on each type of targets with typical examples.

3.1 Monitoring pH

SERS sensors can be established for the pH detection of cellular microenvironments. These measurements could be used as biomarkers to detect tumours since solid tumours contain a highly acidic environment due to high glucose metabolism rate and poor vascular perfusion [124, 125]. For example, Liu et al. [84] developed a pH sensor with SERS nanotags using Au nanostars as the plasmonic substrate and para-mercapto-benzoic acid (pMBA) as Ra molecule. This study showed that the SERS signal intensity at 1700 cm^{-1} decreased when changing the pH from 5 to 9 because this peak was involved with the protonated state of the pMBA molecule. On the contrary, the SERS peak intensity at 1014, 1136, or 1390 cm^{-1} increased when changing the pH from 5 to 9, as those peaks were involved with the deprotonated state of the pMBA. This work indicates that SERS nanotag can be a sensitive tool to monitor structural changes due to local pH environment.

SERS based pH sensing has also been applied in live cells. Kneipp and co-workers developed a mobile and

Table 1 Summary of SERS nanotags for biosensing, including pH, proteins, nucleic acids, and other disease relevant biomarkers

Target	Particle	Range/sensitivity	Application	References
pH	Au-(4-MPy)-BSA (AMB)	pH 4.0–9.0	NIH/3T3 cells	[80]
	Ag NPs with pMBA	pH 2.0–12.0	pH buffers	[81]
	Ag-MBA@SiO_2	pH 3.0–6.0	Macrophage cells	[82]
	AuNP with MBA	pH 6.0–8.0	Live single cells	[83]
	Au nanostars with pMBA	pH 5.0–9.0	pH buffers	[84]
	Au@Ag NPs with carbon nanotubes	pH 3.0–14.0	Live cells	[85]
	Au nanoaggregates with pMBA	pH 2.0–8.0	Live cells	[86]
	Au nanoaggregates with pMBA	N/A	Live cells	[87]
	4-MBA-coated AgNP	pH 6.0–8.0	CHO cells	[88]
	$Cr(CO)_3$–ATP-Au	pH 3.0–9.0	Urine sample	[89]
Proteins	Au-Gr-FON with hairpin-DNA strands	2.67–60 attomoles	PB1-F2 protein	[90]
	AgNP-protein-BSSC thin film	LOD 0.1 ng/mL	FITC- protein	[91]
	3D cavity plasmonic nanoantennas	LOD 300 aM	Protein A and IgG	[92]
	TRF@MIP@GNR aggregates	LOD 10^{-8} mol/L	HSB	[93]
	Fe_3O_4@SiO_2@Au	LOD 5 fg/mL	Human IgG	[94]
	Fluorescence Au/Ag nanoshells	10 fg/mL (sensitive)	HER2	[95]
	AuNPs	10 fg/mL (sensitive)	Cancer proteins	[96]
	AuNR–AuNP	EF ~ 10^7	a-thrombin protein	[97]
	SERS NP clusters	LOD ~1–10 pg/mL	Antigens EHI	[98]
	AuNPs	LOD 0.012 ng/mL	PSA markers	[99]
Nucleic acids	MS immobilized on Nanowave/MFON	N/A	RSAD2 gene	[100]
	NPG disk with MS hairpin probes	LOD 20 pM	ERBB2 gene	[101]
	Au nanoplate films with PVP	LOD 10^{-6} mg/mL	DNA	[102]
	Oligonucleotidemodified Ag NPR	10^{-11}–10^{-8} M	Target DNA	[103]
	$MgSO_4$-aggregated Ag colloid	Specificity of 94.1%	Serum RNA	[104]
	Rod-shaped AuNPs with miR-21 probe	LOD 0.36 nM	miR-21	[105]
	AuNPs	LOD 0.043 Pm	KSHV	[106]
	SERS via LCR	10% changes	DNA methylation	[107]
	SERS via PCR	0.1% of target	DNA mutations	[108]
	AuNPs	Sensitivity, 200 zmol	RNA	[109]
Others (glucoses, metal ions,metabolites, lipids,pathogens)	MBA-Ag@AuNPs-GO	2–6 mM	Glucose	[110]
	AgFON	0–250 mM	Glucose	[111]
	SERS metal carbonyl probe	N/A	Glucose	[112]
	AuNPs/rGO	LOD 0.1 nM	Hg^{2+}	[113]
	Ag with PAR	LOD ~ 522 ppb	Hg^{2+}	[114]
	AuNPs	LOD 20 nM	Hg^{2+}	[115]
	AgNPs	LOD 10, 1 pM	Cu^{2+}, Hg^{2+}	[116]
	AgNPs with microfluidic platform	LOD 0.5 μM	Metabolite	[117]
	SERS with metal nanodomes	N/A	Metabolite	[118]
	AuNPs	LOD 100 nM	Metabolite	[119]
	Ag hydrosol/DMTAP system	LOD ~ 0.3 μM	DMTAP lipid	[120]
	Au nanoshells	N/A	Lipid bilayers	[121]
	SERS and DCDR	~0.3 μM	DMTAP lipid	[120]
	AuNPs	N/A	Bacterias	[122]
	AgNSs	10 CFU/mL	Pathogens	[1]
	MNPs@SiO_2	LOD 10^3 CFU/mL	Pathogens	[123]

biocompatible pH sensor (Fig. 2A-a) using small nanoaggregates of Au colloidal particles with pMBA as reporter which can offer a pH sensitive SERS signature [86]. They introduced this pH sensor into live cells and detect the pH in the surrounding endosome. Figure 2A-b depicts the situation of an NIH/3T3 cell after 4.5 h incubation with the pH sensor. As shown by the photomicrograph, numerous AuNPs accumulated in the cell, enabling pH sensing in different endosomes over the entire cell. Figure 2A-c shows the pH map of the cell displayed as false colour plot of the ratios of the SERS lines at 1423 and 1076 cm^{-1}. Figure 2A-d shows the typical SERS spectra collected using 830 nm cw excitation (3 mW) in the endosomal compartments with different pH value. This study demonstrated pH imaging in single live cells at subendosomal resolution using SERS pH sensors is feasible [81]. Kneipp's group did a further research to monitor changes in local pH of the cellular compartments of living NIH/3T3 cells [87] and found that SERS nanosensors could dynamically monitor the change of local pH in individual live cells to be followed at subendosomal resolution in a timeline of cellular processes.

Furthermore, SERS pH sensors have been proposed for chemical sensing. For example, Talley and co-workers demonstrated that individual functionalized NP clusters could provide a unique platform for chemical sensing based on their SERS response [88]. It was found that 4-MBA-functionalized NPs displayed a distinct response to the pH in the relevant range of biological systems. This makes the SERS pH sensors useful for intracellular chemical measurements. Figure 2B-a shows the SERS response of a 4-MBA-coated NP as a function of pH, normalized to the ring-breathing mode and Fig. 2B-b shows the normalized peak height for the COO - mode plotted against the pH of the bulk solution, indicating that this 4-MBA-functionlized NPs are sensitive to pH changes in a biologically relevant pH range.

In order to achieve higher sensitivity and wider pH testing range, some new attempts have been made. For instance, Kong et al. used a new Ra molecule, arene chromium tricarbonyl linked aminothiophenol ($Cr(CO)_3$–ATP), conjugated with nano-roughened planar substrates coated with Au, to develop SERS based pH sensor [89]. The $Cr(CO)_3$–ATP reporter provides the advantage of monitoring the pH dependence using the strong CO stretching vibrations in the mid- range of 1800–2200 cm^{-1}, while Raman intensity of the CO stretching vibrations at ~ 1820 cm^{-1} strongly depends on the pH of the environment. This SERS pH sensor can

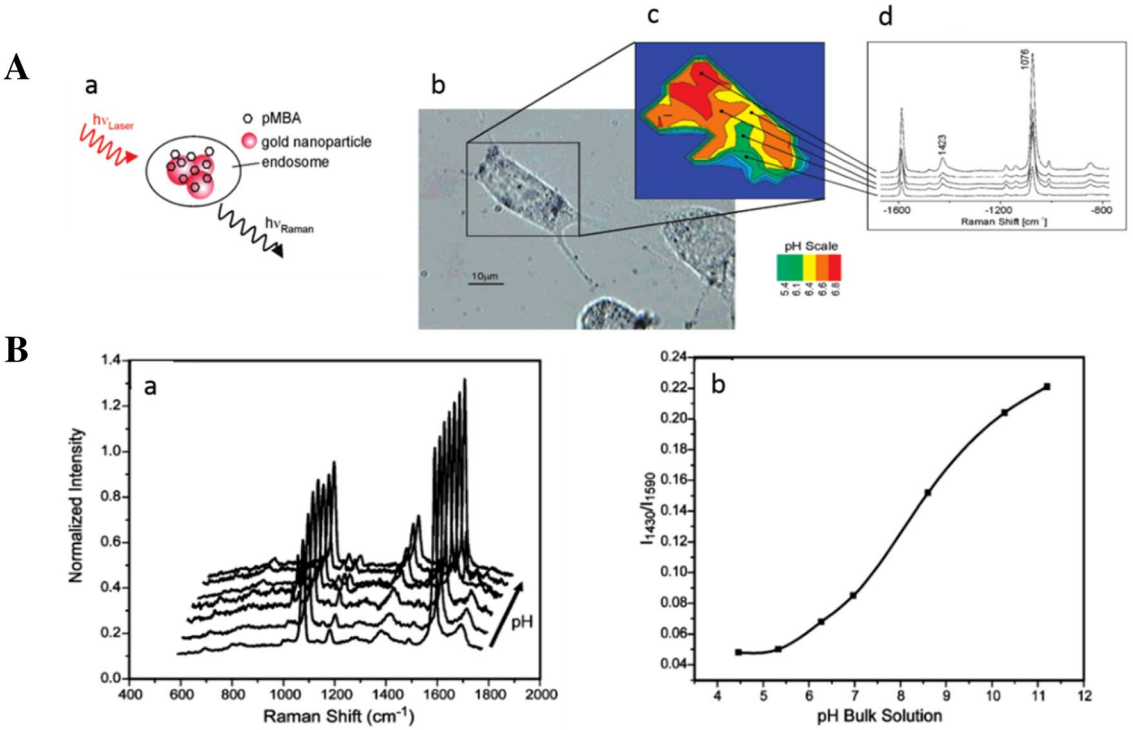

Fig. 2 Probing and imaging pH values in individual live cells using a SERS nanosensor. Schematic of optical pH probing (**A**-a), photomicrograph of an NIH/3T3 cell after 4.5 h incubation with the pMBA Au nanosensor (**A**-c), pH map of the cell displayed as false colour plot of the ratios of the SERS lines at 1423 and 1076 cm^{-1} (**A**-c), typical SERS spectra collected in the endosomal (**A**-d); SERS response of a 4-MBA-coated nanoparticle as a function of pH, normalized to the ring-breathing mode with different pH (**B**-a), normalized intensity for the carboxylate stretching mode plotted against the pH of the bulk solution (**B**-b). Cited from Ref. [86] and [88]

successfully detect the pH in the range of 3.0–9.0. They also demonstrated the effectivity of this pH sensor by measuring urine sample, which has high ionic strength and the data closely correlated to the value obtained from conventional sensor. These pH-sensing approaches thus could be used for future biomedical applications.

3.2 Protein Biomarkers

Measurement of biomarkers in blood such as protein biomarkers is commonly considered as a simple way to screen patients and also enable routine monitoring. Porter and co-workers developed SERS-based sandwich immunoassay platform (Fig. 3A) for protein biomarkers, providing a sound basis for the development SERS-based immunoassay. Three key components were proposed in their SERS-based immunoassay platform: [1] use of a capture substrate to specifically extract and concentrate antigens from solution; [2] selective tagging of captured antigens with functionalized external SERS nanoparticles; and [3] readout by Raman spectroscopy [126].

Microfluidic based platforms are often employed to conduct SERS-based immunoassay. For instance, Wang et al. developed a rapid and extremely specific SERS

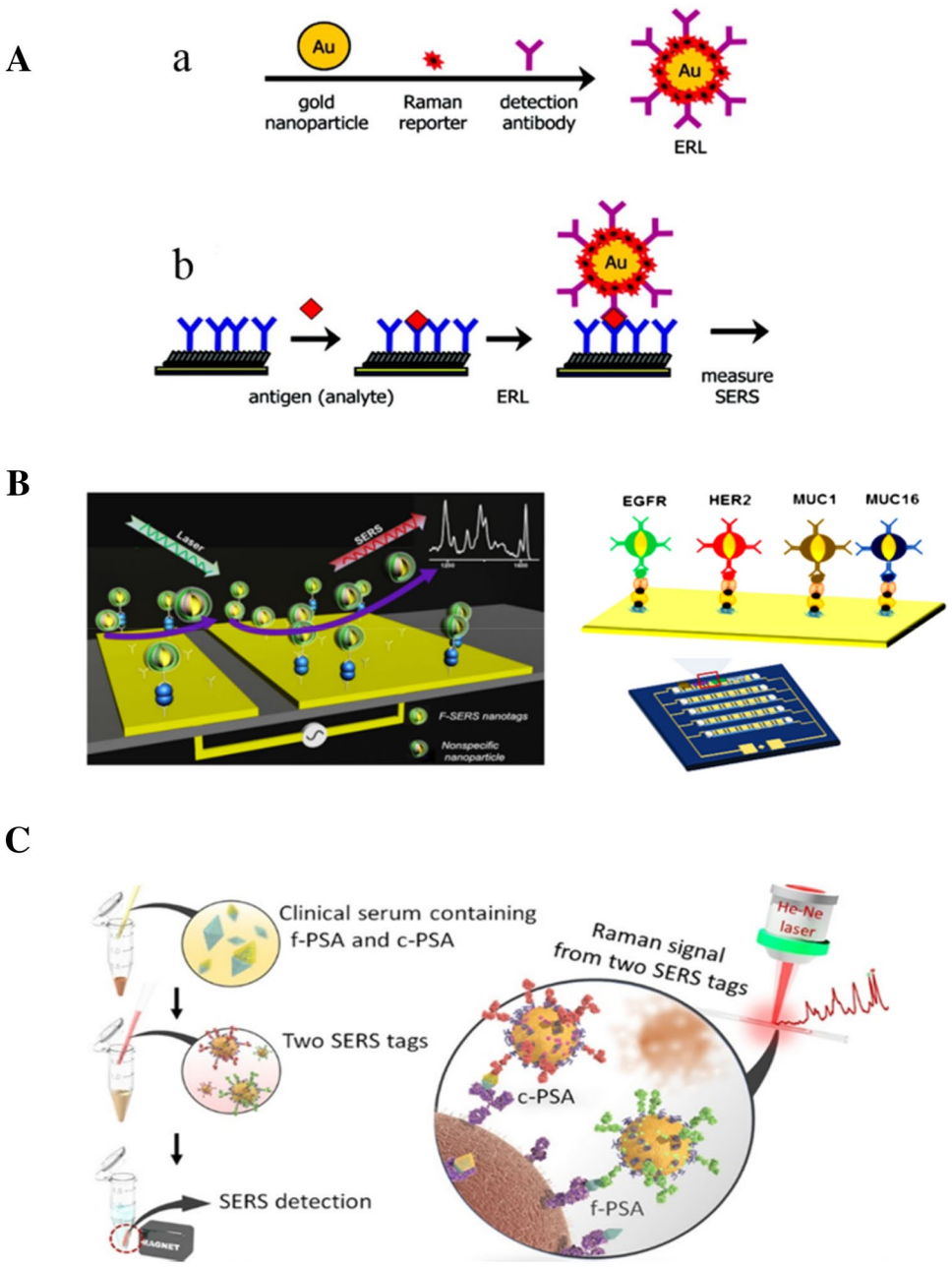

Fig. 3 SERS-immunoassay platform for protein biomarker sensing. Schematic illustration of SERS-based immunoassay platform (**A**); Multiplexed protein biomarker detection using ac-EHD-induced SERS-immunoassay (**B**); SERS-immunoassay using magnetic beads and SERS nanotags (**C**). Cited from Ref. [126], [95], [96] and [99]

immunoassay method using electrohydrodynamic (ac-EHD) force to markedly reduce the assay time and nonspecific binding for breast cancer biomarkers detection (Fig. 3B) [95]. They utilized rational-designed fluorescence-integrated Au/Ag nanoshells to monitor the capture performance and associated nonspecific binding. The results showed that the assay time with ac-EHD SERS immunoassay was shortened from 24 h to 40 min and 10 times lower than that of the conventional SERS immunoassay with the nonspecific binding. This study demonstrated that the proposed platform was highly sensitive (10 fg/mL) and had great potential to detect protein biomarkers in patient samples. This platform was further developed to simultaneously detect multiple cancer protein biomarkers from clinical samples by using 4 different SERS nanotags [96]. They constructed a microfluidic device containing five individual microchannels with each channel comprehending an array of asymmetric electrode pairs (Fig. 3B). This microfluidic device was successfully used for simultaneous capture and multiplexed detection of 4 different protein biomarkers, human epidermal growth factor receptor 2 (HER2); Mucin 1, cell surface associated (MUC1); epidermal growth factor receptor (EGFR); and Mucin 16, cell surface associated (MUC16). The proposed approach with the ability to simultaneously detect four individual cancer biomarkers within each channel has great potential to be developed as a useful tool for a broader panel of cancer biomarkers.

Pulling-down immunoassay by using magnetic beads and SERS nanotags is another platform for protein biomarker detection. To improve the diagnostic performance of prostate cancer, Cheng and co-workers developed a SERS-based immunoassay to determine free to total (f/t) prostate specific antigen (PSA) ratio using the pulling-down immunoassay [99]. The schematic representation for this technique is illustrated in Fig. 3C. They performed this assay to simultaneously detect dual PSA markers, free PSA (f-PSA) and complexed PSA (c-PSA to assess the clinical applicability. The outcomes for f/t PSA ratio exhibited a good linear correlation with results measured by the electrochemiluminescence (ECL) system. They also applied this approach to detect f-PSA and c-PSA in 13 clinical serum samples, showing better precision than parallel assays.

Taking advantage of SERS hot spots and the optical property of AuNRs, Wang et al. proposed a novel SERS aptasensor based on Au nanorods - Au nanoparticles (AuNR-AuNPs) junctions to detect human a-thrombin in human blood serum [97]. They functionalized AuNRs by anti-thrombin antibody to detect the target α-thrombin protein and labelled the citrate stabilize AuNPs by thrombin-binding aptamer (TBA) and Ra molecule (mercaptobenzoic acid, MBA) to create a protein-sandwich between nanorods and NPs for SERS detection. They also used this approach to test complex biological matrix such as human blood serum for practical use. This overall concept could be further developed for multiplex protein assay using different Ra molecules, to establish a SERS platform based on this aptamer-protein recognition and junction formation strategy.

Microfluidic device is used to achieve simultaneous and sensitive detection of some protein biomarkers by using affinity biomolecules, such as monoclonal antibodies (mAbs), which are the current Au standard affinity reagents used for protein biomarker (antigen) detection. However, highly specific mAbs are expensive and time-consuming to isolate and manufacture. A robust and sensitive SERS-based bioassay platform has thus been explored to simultaneously detect two pathogen antigens with low cost and high practicability [98]. Wang et al. constructed the microfluidic device with multiple channels using silica-coated, highly purified SERS NP clusters to enable a rapid and accurate detection of antigens. As a result, this device was successful used for ultrasensitive and specific detection of individual 350 and 030 (*E. histolytica* antigens EHI_115350 and EHI_182030 were called "350" and "030"), achieving with LOD of ~ 1 pg/mL (58.8 fM) and 10 pg/mL (453 fM), respectively. This study provided a powerful analytical platform, holding great potential for high throughput multiplexed detection of protein biomarkers.

These methods can potentially contribute to the advancement of SERS protein biosensing with better robustness and efficiency. Further, these approaches could potentially be used in clinical diagnosis.

3.3 Nucleic Acids

Nucleic acid detection is increasingly popular due to the broadening knowledge of sequence-based pathogen identification, cancerous mutations, and inherited genetic diseases. Wang et al. developed a new class SERS-based lateral flow assay (LFA) to simultaneously detect dual DNA markers as illustrated in Fig. 4A [106]. The LFA strip in this sensor consisted of two test lines and one control line. The researchers used detection DNA probes to label SERS nanotags and quantitatively evaluate the dual DNA markers with high sensitivity. They also employed target DNA, associated with Kaposi's sarcoma-associated herpesvirus (KSHV) and bacillary angiomatosis (BA) to validate the detection capability of this SERS-based LFA strip. The LOD for KSHV and BA, determined by method, were estimated to be 0.043 and 0.074 pM, respectively. These data were around 10,000 times higher sensitivity than experimental data using the aggregation-based colorimetric approach before.

Single DNA base change such as aberrant DNA methylation epigenetic changes, single nucleotide polymorphism (SNP) and point mutation are common events in cancer. It is clinically useful to screen such single DNA base change for disease diagnosis and the selection of the suitable therapies.

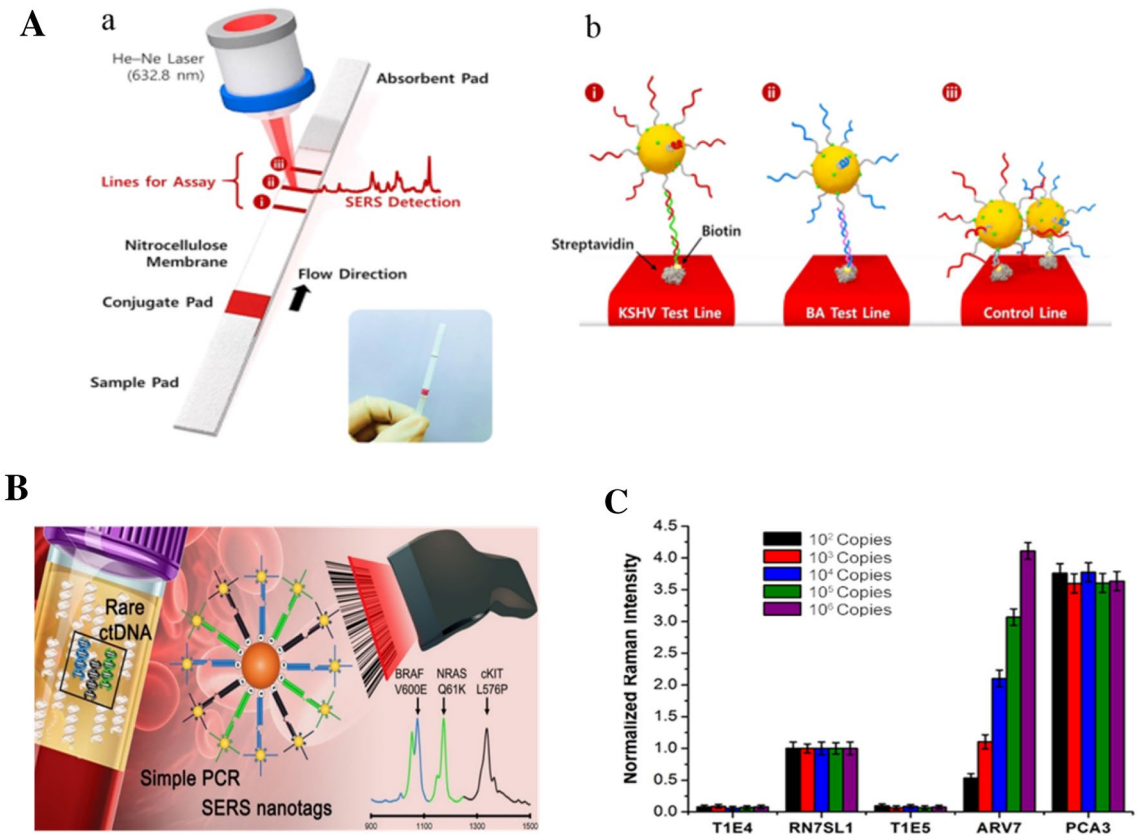

Fig. 4 SERS based detection of Nucleic acid biomarkers. Schematic illustration of the LFA biosensor (**A**); Schematic illustration of SERS nanotags with PCR (**B**); Corresponding normalized Raman intensities for different copy numbers of RNA (**C**). Cited from Ref. [106], [108] and [109]

Wang et al. explored a proof-of-concept research with SERS nanotags via ligase chain reaction (LCR) for multiplexed single DNA base change detection [107]. Methylation can be detected with as low as 10% differences using this method, demonstrating the great potential of SERS for sensitive genetic monitoring. They also successfully applied this assay method to breast cancer cell lines and a serum-derived DNA sample, demonstrating its feasibility on complex biological samples. These assay results were also validated by Next Generation Sequencing, showing its potential for accurate genetic biomarker detection. As current approaches have limitations in multiplex detection, sensitivity and requirement of expensive specialized equipment, an assay taking advantage of the multiplexing and high sensitivity of SERS with the simplicity of standard PCR (Fig. 4B) were further developed [108]. This novel method could reproducibly detect target sequences as low as 0.1% (10 copies, CV < 9%), thus indicating the high sensitivity of the approach. This approach was also successfully employed to specifically detect three important melanoma mutations in multiplex, genotype cell lines and ctDNA from serum samples.

Apart from DNA biomarkers, the analysis of RNA biomarker in cancer can also inform on disease pathogenesis, medical diagnosis, disease staging, and therapeutic monitoring. Reverse transcription-recombinase polymerase amplification (RT-RPA) is a viable alternative to traditional real-time polymerase chain reaction (RT-PCR) techniques for the RNA biomarker level detection. A five-plexed assay developed by Koo et al. was described for simultaneously detecting promising next-generation RNA biomarkers in PCa within 80 min [109]. This assay involved the use of multiplexed isothermal RT-RPA to amplify RNA targets in the sample before labelling the amplicons with different synthesized SERS nanotags for rapid one-pot SERS detection. The test of clinical urine and tissue specimens demonstrated this method was capable of highly sensitive (200 zmol) and specific PCa molecular profiling. Figure 4C shows the corresponding normalized Raman intensities for different copy numbers of five different target RNAs, which were detected using this approach. The application of this platform were further explored in the clinic samples [104].

3.4 Other Biomarkers

3.4.1 Glucose

Glucose is a key metabolite in living organisms, especially in patients suffering from diabetes, which affects 10.7% of Americans over the age of 20 and 23.1% of those over the age of 60, according to the National Institutes of Health [127]. Diabetics are often needed to check their blood glucose levels 3–10 times/day [34]. Thus, it will be greatly useful for diabetic patients if there is an in vivo glucose sensor which enables real-time measurement of blood glucose levels without drawing blood. Historically, glucose has been difficult to detect by SERS because its normal Raman cross section and weak or no adsorption to bare Ag surfaces. Van Duyne's group reported the first systematic study of the direct detection of glucose using SERS [111]. They partitioned glucose into an alkanethiol monolayer adsorbed on an Ag film over nanosphere (AgFON) surface, thus it was pre-concentrated within the 0–4 nm thick zone of EM field enhancement. By employing this leave-one-out partial least-squares (LOO-PLS) method, they demonstrated quantitative glucose detection both over a large (0–250 mM) and clinically relevant concentration range (0–25 mM).

Kong et al. [112] used a transition metal carbonyl probe to develop a highly specific and sensitive SERS-based assay for glucose detection. This assay did not need the conjugation of the metal carbonyl probe and a SERS-active species, it utilized the CO stretching vibrations of the metal carbonyl, which lied in a silent region of the SERS spectrum (1800–2200 cm^{-1}), for quantification. High selectivity for glucose was demonstrated in this work. They also detected a human urine sample doped with glucose using this method to demonstrate its capability of glucose testing. These results are highly promising for the SERS-based in vivo glucose detection.

3.4.2 Metal Ions

Detection of metal ion like lead (Pb^{2+}), a common environmental contaminant, is crucial to human health and environmental monitoring. Grane et al. reported a SERS based method to detect Pb^{2+} ions with a 4-(2-pyridylazo) resorcinol (PAR) coating modified with a disulphide on a roughened silver substrate [114]. The limit of detection (LOD) was ~ 522 ppb, but the selectivity seemed to be a big problem for this approach. Wang et al. thus proposed a unique and simple SERS nanotag to detect Pb^{2+} ions based on the DNAzyme concept [115]. They accomplished the conjugation of AuNPs with DNA and Ra molecules. Upon binding of Pb^{2+} ions to the substrate, a proportional amount of AuNPs conjugates would be cleaved from the Au surface, resulting in Raman signal decrease. Thus, this method realizes a sensitive and specific SERS DNAzyme biosensor for the detection of Pb^{2+} ions. This biosensor can detect as low as 20 nM Pb^{2+} ions, owing to the high sensitivity of SERS.

Meanwhile, Li and co-workers developed a different method for the ultrasensitive detection of Cu^{2+} and Hg^{2+} using cysteine-functionalized AgNPs linked with Raman-labelling molecules [116]. The AgNPs co-functionalized with cysteine and 3,5-Dimethoxy-4-(6′-azobenzotriazolyl) phenol (AgNP conjugates) were utilized to detect Cu^{2+} and Hg^{2+} based on aggregation-induced SERS effect. This approach showed an unprecedented LOD of 10 pM for Cu^{2+} and 1 pM for Hg^{2+}, of which, the LOD were a few orders of magnitude more sensitive than the typical colorimetric approach. Thus, the study in this research area can provide general and simple approaches for the detection of other metal ions.

3.4.3 Drug Metabolites

SERS has the potential to allow real-time drug and metabolite monitoring which can help physicians in deciding dosage amounts and time intervals tailored to the individual's biochemistry. As reported by Cunningham and co-workers, a SERS sensor comprised of an array of closely spaced metal nanodomes was incorporated into the flexible tubing, which commonly used for IV drug delivery and urinary catheters [118]. The nanodome sensor was prepared by a low-cost, large-area process that enables single use disposable operation. This study demonstrated that the fabricated sensor can be used to kinetically detect promethazine (pain medication) and urea (urinary metabolite) within the clinically relevant concentration range, which would increase the safety of intravenous (IV) drug injection and point-of-care health monitoring, if it is being applied to clinic.

Yang and co-workers used Au NPs dotted magnetic nanocomposites (AMN) modified with inositol hexakisphosphate (IP6) as SERS substrate to quickly monitor drug-related biomarkers in saliva and to trace on-site screen drug biomarker in fingerprints [119]. The substrate presented a huge SERS activity by inducing with an external magnet. The LOD of the drug biomarker in fingerprint reached 100 nM by using this method. Furthermore, a portable Raman spectrometer conducted this AMN-based SERS assay approach successfully, which may be used to on-site and accurately differentiate between the smokers and drug addicts in the future.

3.4.4 Lipids

In biology, lipids act as structural elements of cell membranes, a form of energy storage, fats in adipose tissue and important signalling molecules, being crucial for human health. In a research by Halas and co-workers, the interaction between a small molecule drug (ibuprofen) with Au nanoshells was

studied using SERS and IR spectroscopy [121]. The interaction of ibuprofen with lipid bilayers in the gastrointestinal tract is one of the mechanisms of observed ibuprofen side effects, such as gastrointestinal bleeding. The spectroscopic results revealed specific interactions between ibuprofen and phospholipid moieties and indicated that the overall hydrophobicity of ibuprofen played an significant part in its intercalation in these membrane mimics.

Simokova and co-workers reported a detection method for 1, 2-dimyristoyl-3-trimethylammonium-propane (DMTAP) lipid by employing two Raman techniques with improved sensitivity: drop coating deposition Raman (DCDR) and SERS spectroscopies [120]. The dried ring SERS spectra of Ag hydrosol/DMTAP system were obtained down to ~ 0.3 μM DMTAP concentration using this method, meaning the sensitivity of SERS was about five orders of magnitude higher than that of conventional Raman spectroscopy. Using SERS for the study of lipids is a developing field and expanding the types of lipids studied could have important impacts in membrane and lipid biology.

3.4.5 Pathogens

The identification and timely detection of pathogenic bacteria in food is important because many diseases are caused by bacterial infection or contamination [128]. A novel monodispersed silver nanospheres (AgNSs) has been developed to sensitively detect multiple pathogens by the assembly of silver nanoclusters (AgNCs) through a bottom-up assembly [1]. Wang et al. used the synthesized SERS substrate for bacteria detection at a low concentration of 10 CFU/mL with great signal reproducibility. They also accomplished differentiation of three key pathogens (*E. coli* O157, *S. typhimurium*, and *S. aureus*) including live and dead cells, using canonical variate analysis (CVA) in conjunction with Raman spectra.

Furthermore, an immunomagnetic SERS biosensor was developed to detect two key pathogens, *Salmonella enterica serovar Typhimurium* and *Staphylococcus aureus* by using newly designed silica-coated magnetic probes and SERS nanotags [123]. They could detect the pathogen at cell concentration of 10^3 CFU/mL, demonstrating high sensitivity and specificity of the SERS nanotag for pathogen detection. Selecting appropriate Raman labels and SERS substrate, these SERS-based pathogen detection platforms could be evolved to monitor raw and processed foods to assure the food safety.

4 SERS Bioimaging

SERS-based bioimaging holds the potential to be an important diagnostic tool to complement other imaging techniques such as fluorescence imaging, owing to its unique advantages other methods may lack. It can provide clinically relevant information under in vitro, in vivo and ex vivo conditions, offering the decisive advantages. In this section we will discuss the development of SERS bioimaging in different conditions as summarized in Table 2 and then highlight the SERS applications in each condition, respectively.

4.1 In Vitro SERS Imaging Applications

In vitro detection of biomarkers in cancer models, tissue samples and cell lines using SERS nanotags, constructed with reporter molecules is studied by many researchers.

Dinish et al. established three multiplexing capable, biocompatible SERS nanotags for the multiplex detection of three intrinsic cancer biomarkers–EGFR, CD44 and TGFβRII in a breast cancer model [132]. They injected three bioconjugated SERS nanotags (MGITC, Cy5 and Rh6G in the ratio 1:1:2) into the centre of the tumor on a subcutaneous MDA-MB-231 breast cancer xenograft mouse model. Figure 5A-a shows the multiplexed SERS spectra measured from the cell surface, while Fig. 5A-b provides the bright field image of the cells. It is clear that the cell surface spectra obviously exhibit the unique spectral peak from each SERS nanotags, allowing biomarkers multiplex detection. Relative distribution of the intrinsic cancer biomarkers on the cell surface is obtained by mapping at respective Raman peaks of the SERS nanotag to confirm the specific interaction and binding of the conjugated nanotags to the three biomarkers on cell surface in Fig. 5A (c-e). Raman mapping was carried out for all three nanotags at a depth interval of 2.5 μm to validate the binding of the nanotags to the cell surface. A typical image stack mapped for Cy5 nanotag conjugated to TGFβRII is showed in Fig. 5A-f. Thus, simultaneous detection of multiple biomarkers has tremendous potential in increasing the sensitivity and diagnostic accuracy of various cancers.

Yuan and co-workers integrated near-infrared (NIR) responsive plasmonic Au nanostars with resonant dyes for multiplexed SERS bioimaging [133]. Xiao et al. cultured the cells on silicon wafers or glass slides coated with the Ag NP films, then labelled the cultured cells with Aha and treated with precursors functionalized with a bioorthogonal Ra molecules [134] (Fig. 5B). They used the self-assembled AuNPs arrays and successfully visualized the newly synthesized proteins, glycans, and lipids on cell surfaces, demonstrating SERS bioimaging of various membrane molecules by employing various Ra moleucles such as azides, alkynes, and C–D bonds. Multi-color SERS bioimaging by using reporters with different Raman frequencies will be valuable to simultaneously visualize multiple biomolecules. Complementary to fluorescence imaging and label-free imaging, this method offers another way for live-cell microscopy.

Table 2 Summary of SERS nanotags for bioimaging

Types	Particles	Targets	References
In vitro imaging	Monodisperse Au nanostars	Tumor suppressor	[129]
	SERS NPs with antibodies	Tissue specimens	[130]
	Mycosynthesized AgNPs, phytosynthesized AgNPs	Carcinoma cells	[131]
	Bioconjugated SERS nanotags	EGFR, CD 44, TGFßRII	[132]
	Ag island film with AuNPs	Proteins, glycans, lipides	[134]
	Folate-targeted SERS nanoprobe	Cancer cells	[148]
In vivo imaging	Au nanorods coated with silica/polymer mutilayers	Tumor	[135]
	AuNPs with silica shell	Precancerous lesions	[136]
	Upconversion fluorescence SERS dual mode tags	Live cell	[137]
	Au nanostar probe	Tumor	[138]
	AuNPs with silica and PEG shell	Dorsal mouse skin	[139]
	AuNPs	zebrafish embryo	[140]
	AuMN-DTTC	Mouse	[141]
	Folate receptor SERRS NPs	Tumor lesions	[149]
Ex vivo imaging	AuNPs-silica with affibodies	EGFR	[142]
	Au–silica NPs	EGFR-positive tumor	[143]
	(4-MBA)-labelled Au/Ag core–shell bimetallic NPs	Nasopharyngeal tissue	[144]
	Hollow AgNP	PSA in epithelial tissue	[145]
	Hollow Au nanospheres	Breast cancer cells	[146]
	Ag/Au nanorods	Tumor cells	[147]

Recently, Liu et al. developed a new folate-targeted SERS nanotag for selective bioimaging and diagnosis of FR-overexpressed cancer cells [148]. They anchored the monolayer coverage of Raman-active azide derivatives at the surface of AuNPs to increase the number of label molecules and further highly conjugated with folate cyclooctyne derivatives by the copper-free click reaction. These developed SERS nanotags can selectively bind to the FR-positive cancer cells, and the dark-field and the obtained SERS bioimages can show the distribution of the nanotags in typical cancer cells with different levels of FRs, giving the distinguishable images between the FR-positive cells and the FR-negative cells. This method indicates high potential to be ideal bioimaging agents for tumor targeting and therapeutics.

4.2 In Vivo Imaging Applications

SERS techniques have advanced towards microscopy and small-animal in vivo imaging applications. Although SERS technologies can be used to image Raman fingerprints in single cancer cells, and associated gene expression for physiological states and phenotypes detection, SERS based cancer imaging mainly depends on the recognition of known markers by the generated immunocomplexes [29]. Moreover, SERS provides great resolution for intracellular microenvironments monitoring and the cellular distribution tracking of extrinsic molecules.

For example, zebrafish embryo has been utilized as a good model to study the distribution of NPs during its development using SERS imaging, as reported [140]. Wang et al. microinjected SERS nanotags comprising AuNPs and nonfluorescent Raman labels into zebrafish embryos at the one-cell stage. Then, Raman mapping was used to evaluate their distribution in different types and tissues of developing embryo at five different stages between 6 and 96 hpf (hours post-fertilization). Figure 6A shows the optical image and SERS intensity maps of C–C vibration band from SERS NPs at 1078 cm^{-1} in the body musculature of the zebrafish embryo. This technique was further used to detect multiplex SERS NPs in vivo, indicating that multiple labels can be detected by Raman mapping in undifferentiated cells as they develop into distinct cell- and tissue-types. Moreover, the biocompatibility and toxicity studies showed that the NPs were not toxic and the embryos exhibited normal morphological and gene expression.

Designing contrast agents for multimodal imaging is an emerging and important field. Any given imaging method could be powerful in certain aspects and weak in others. Thus, combining two or more modalities may allow the offsetting of one modality's weakness with the strength of another [29]. Yigit and co-workers reported a novel nanomaterial (AuMN-DTTC) that can be used as a bimodal contrast agent for in vivo magnetic resonance imaging (MRI) and Raman spectroscopy (Fig. 6B) [141]. This novel nanomaterial consisted of MRI-active superparamagnetic iron oxide

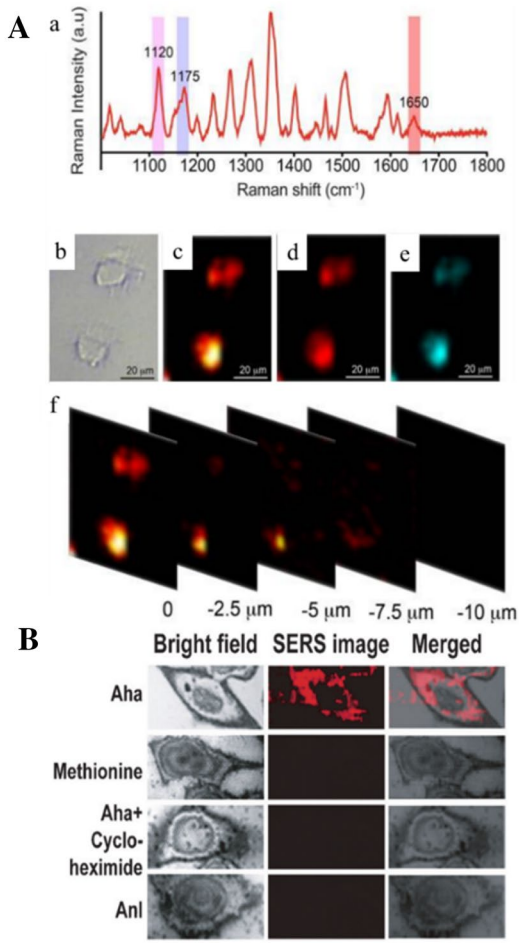

Fig. 5 In vitro SERS imaging. Multiplexed SERS spectra measured from the cell surface and SERS mapping of nanotags and biomarkers (**A**); SERS imaging of the newly synthesized proteins labelled with Aha, Methionine-, cyclohexi- mide-, and Anl-treated cells (**B**). Cited from Ref. [132] and [134]

NPs, and Au nanostructures, wherein, the Au served as an enhancement for a Raman active dye molecule to generate SERS signal. They also proved synthesized nanostructure that could be used as a SERS active material both in silico (in aqueous solution) and in vivo. This is the first study that reports the combination of a SERS nanotag and MRI imaging for in vivo imaging application.

As molecular imaging moves towards lower detection limits, the elimination of endogenous background signals becomes imperative. Mallia and co-workers [139] developed a simple and economical filter-based method, which can significantly reduce the intrinsic background signals in wide-field SERS imaging. Specifically, it can segregate the signal from SERS NPs from the tissue autofluorescence background in vivo by using specific narrow-band filters. As SERS NPs have extremely narrow spectral peaks and do not overlap significantly with endogenous Raman signals, SERS NPs can be explored to image picomolar (pM) concentrations of NPs against a broad tissue autofluorescence background in wide-field modewith short integration time, because SERS NPs have extremely narrow spectral peaks and do not overlap markedly with endogenous Raman signals. Figure 6C shows SERS bandpass images of 40 pM SERS-active AuNPs in solution. Figure 6C (a) is white light image showing the laser irradiation volume, and (b) to (d) are SERS bandpass images centering at 890, 900, and 910 nm, respectively. This technique is expected to facilitate further development of SERS-based contrast agents for molecular imaging in vivo.

Currently, it is not possible for surgeons to visualize microscopic implants clinically, which impeded the tumor removal and leading to tumor recurrences and poor outcomes in most patients. Therefore, it is in urgent need of new intraoperative imaging approaches that can overcome this difficulty. Oseledchyk and co-workers developed a technique using folate receptor (FR)-targeted surface-enhanced resonance Raman scattering (SERRS) NPs, as the folate receptor was typically overexpressed in ovarian cancer [149]. This method made use of the ratiometric information resulting from the differential homing of anti- folate receptor SERRS NPs and non-targeted SERRS NPs. Furthermore, the abdomen of healthy and tumor-bearing mice were imaged and successfully enabled the detection of tumor lesions. The obtained map can be visualized in a simplified manner for surgical guidance. They also demonstrate the accuracy of this imaging technique with BLI and histology, showing high potential for clinical translation.

4.3 Ex Vivo Imaging Applications

The ex vivo imaging of biopsied tissues using SERS techniques was reported for the first time in 2006 on prostate cancer tissues [145]. In 2012, Chen et al. used Au/Ag core–shell NPs as SERS substrates and 4-mercaptobenzoic acid (4-MBA) as Ra molecule to detect LMP1 in ex vivo nasopharyngeal tissue specimens [144]. The in situ detection of LMP1 in normal and cancerous nasopharyngeal tissue sections is shown in Fig. 7A. The typical SERS spectrum obtained from cancer tissue exhibits a strong Raman signal, due to specific binding of the LMP1 antibody, whereas only negligible SERS signals are observed in normal tissue, likely due to nonspecific adsorption of the LMP1-SERS nanotags. It is shown in Fig. 7A that normal nasopharyngeal epithelial tissue exhibits as black almost everywhere with only few dark red spots appear (possibly due to nonspecific conjugating of the LMP1 antibody), demonstrating that there is no expression of LMP1, whereas cancer cells show as yellow and white, demonstrating the high expression of LMP1 in nasopharyngeal cancer cells. This method showed high sensitivity and specificity.

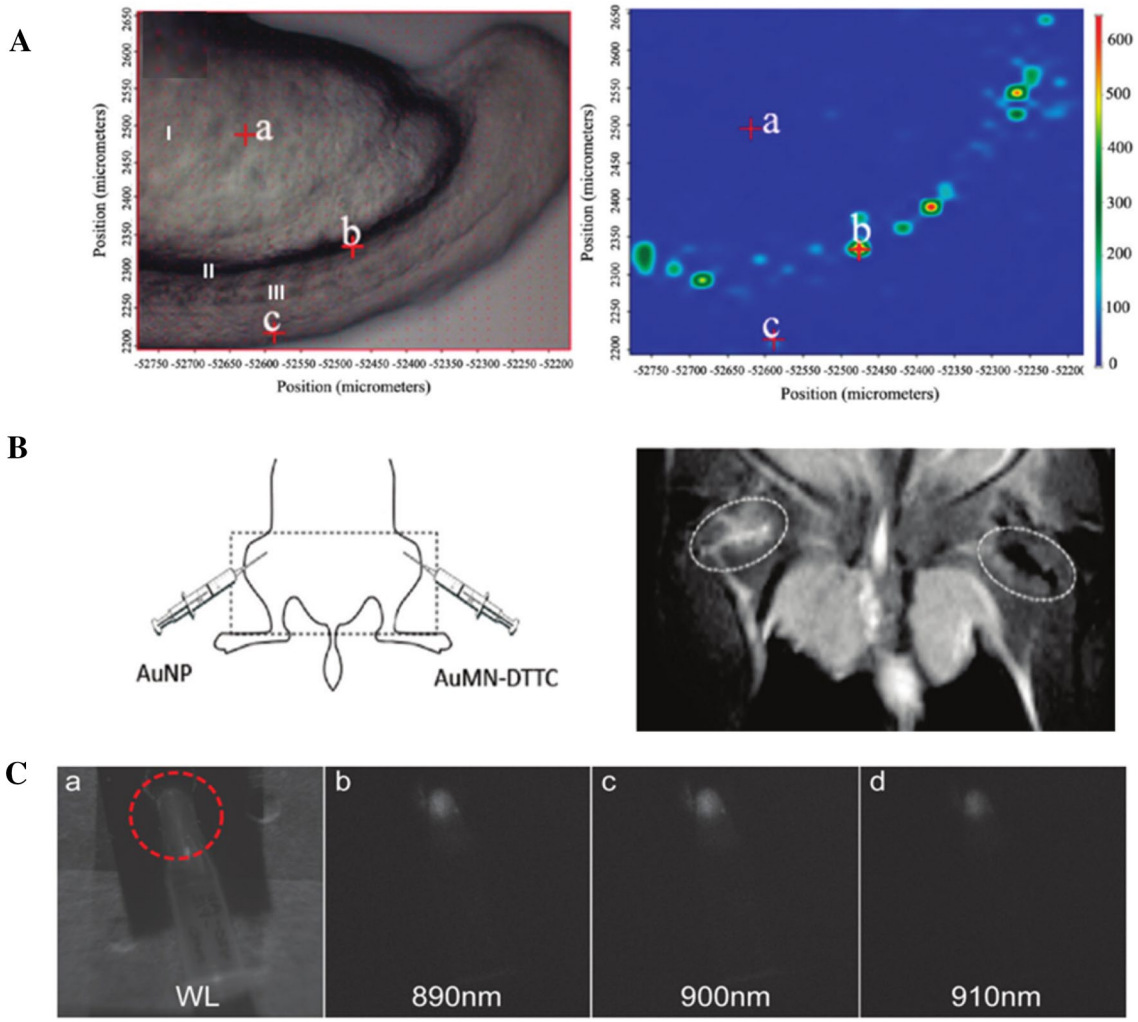

Fig. 6 In vivo SERS imaging. The optical image and SERS intensity maps of C–C vibration band at 1078 cm^{-1} from SERS NPs in the body musculature of the zebrafish embryo (**A**); in vivo MR image of mouse injected intramuscularly with AuMN-DTTC and AuNP (**B**); SERS band-pass images of 40 pM SERS-active AuNPs in solution (**C**). Cited from ref [140], [141] and [139]

Lee and co-workers reported a SERS-based cellular imaging method for detection of breast cancer phenotypic markers expressed on cell surfaces ex vivo [146]. This method involved the synthesis of SERS nanotags including silica-encapsulated hollow Au nanospheres (SEHGNs) linked with specific antibodies. Hollow Au nanospheres (HGNs) increased individual particle SERS intensity by localizing surface EM fields through pinholes in the hollow particle structures. This capacity made HGNs possible to detect specific biological markers expressed in cancer cells. Furthermore, silica encapsulation markedly enhanced the stability of NPs. They used this approach for three breast cancer cell phenotypes multiplex imaging. Expression of epidermal growth factor (EGF), ErbB2, and insulin-like growth factor-1 (IGF-1) receptors were also evaluated in the MDA-MB-468, KPL4 and SK-BR-3 human breast cancer cell lines (Fig. 7B).

Ex vivo imaging has also been employed for the identification and characterization of circulating tumor cells (CTC) in unprocessed human blood. Nima and co-workers introduced a new technique for the highly specific multiplex detection of tumor cells in unprocessed whole human blood using SERS nanotags. These SERS nanotags consisted of silver-decorated Au nanorods, four Raman molecules and four antibodies (-anti-EpCAM, anti-IGF-1 Receptor β, anti-CD44 and anti-Keratin18) [147]. In order to distinguish these molecules, the researchers assigned different colors for the individual peaks of the four organic molecules' spectra. As it can be seen from Fig. 7C, the four colors superimpose on the optical images of a cell, obviously showing that the cell is a CTC. This method offered a way to detect a single cancer cell within 7 millions of blood cells with high specificity, as no enrichment or tedious, time-consuming procedures required.

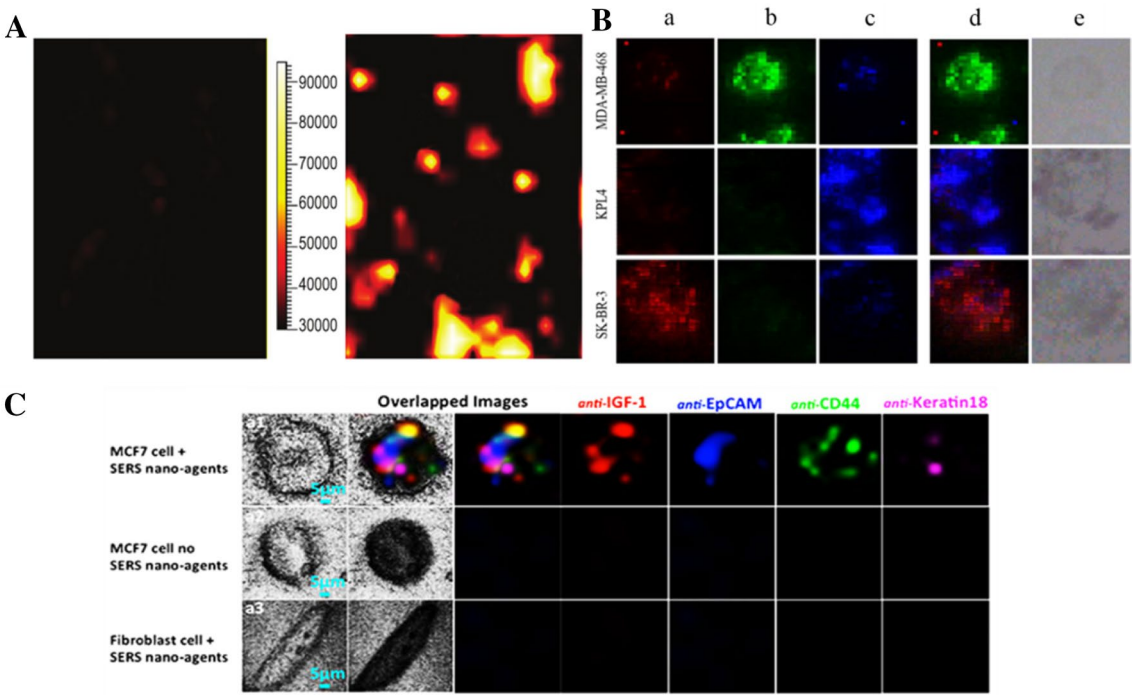

Fig. 7 Ex vivo SERS imaging. SERS images of example of normal tissue and cancerous tissue (**A**); SERS mapping images of corresponding cell lines were measured at *a* 1650 cm^{-1} (RBITC), *b* 1619 cm^{-1} (MGITC), *c* 1490 cm^{-1} (RuITC), *d* Merged SERS mapping images for three different types of breast cancer cells and *f* Bright field images (**B**); transmission and Raman images of a sample containing just one MCF-7 cell among 90,000 fibroblast cells (**C**). Cited from Ref. [144], [146] and [147]

5 Summary and Perspective

In summary, a wide variety of SERS NPs have been reviewed in terms of their plasmonic properties for SERS activity. Furthermore, SERS applications in biosensing and bioimaging in biological samples have been discussed. Owing to their high sensitivity, specificity, virtually unlimited multiplexing capability and photostability of SERS nanotags, SERS based bioassays have progressed greatly towards the simultaneous quantification of multiple biomarkers such as proteins and nucleic acids. In general, the assays only need small sample volumes (a few microliters) and have extremely low detection limits (up to femtomolar level). The capability of SERS bioassays to simultaneously detect multiple biomarkers (such as DNA and protein) in blood, urine and saliva is very important for practical applications such as early and point-of-care diagnostics. Significant advances have also been made in the development of SERS bioimaging. SERS-based bioimaging has shown great potential to make SERS an important diagnostic tool to complement the other imaging techniques, such as magnetic resonance imaging (MRI), fluorescence imaging and computed tomography, owing to its ultra-sensitivity (single molecule/cell) that diagnostic counterparts of many other methods lack. Therefore, it holds great potential to become a primary imaging tool for early disease detection or for the determination of post-operative outcomes with the instrument advancement in the near future.

Detecting the biomarkers and translating SERS signal into a molecular imaging technique or combining it with a biomedical imaging technique can benefit patients dramatically, offering them disease detection at a very early stage. Therefore, a substantial effort needs to be made to transform SERS into a more clinically relevant modality. There are several key challenges that need to be addressed. The first challenge is the limited information or knowledge on the evolution of specific biomarkers during the course and treatment of a disease as well the absence of available targeting moieties that are capable of identifying and attaching them on SERS nanotags. Another important challenge is to discover biocompatible and biodegradable SERS nanotags with minimum cytotoxicity. Finally, to date, most of the SERS biosensing and bioimaging studies with nanoparticles were carried out in cells or tissues, with very few successful examples in live animal models. Much more improvements in biocompatible nanoparticles, SERS biosensing and bioimaging system will still need to be addressed.

Acknowledgements This work was supported by the Australian Research Council (ARC) Discovery Early Career Research Award (DECRA-DE 140101056) to Y.W.

References

1. Wang Y, Lee K, Irudayaraj J. Silver nanosphere SERS probes for sensitive identification of pathogens. J Phys Chem C. 2010;114(39):16122–8.
2. Fleischmann M, Hendra PJ, McQuillan AJ. Raman spectra of pyridine adsorbed at a silver electrode. Chem Phys Lett. 1974;26(2):163–6.
3. Jeanmaire DL, Van Duyne RP. Surface Raman spectroelectrochemistry: part I. Heterocyclic, aromatic, and aliphatic amines adsorbed on the anodized silver electrode. J Electroanal Chem Interfacial Electrochem. 1977;84(1):1–20.
4. Albrecht MG, Creighton JA. Anomalously intense Raman spectra of pyridine at a silver electrode. J Am Chem Soc. 1977;99(15):5215–7.
5. Otto A, Billmann J, Eickmans J, Ertürk U, Pettenkofer C. The "adatom model" of SERS (surface enhanced Raman scattering): the present status. Surf Sci. 1984;138(2–3):319–38.
6. Bruckbauer A, Otto A. Spectroscopy of pyridine adsorbed on Raman single crystal copper electrodes. J Raman Spectrosc. 1998;29:665È72.
7. Arenas JF, Woolley MS, Otero JC, Marcos JI. Charge-transfer processes in surface-enhanced Raman scattering. Franck-Condon active vibrations of pyrazine. J Phys Chem. 1996;100(8):3199–206.
8. Le Ru E, Etchegoin P. Principles of Surface-Enhanced Raman Spectroscopy: and related plasmonic effects. Amsterdam: Elsevier; 2008.
9. Kahl M, Voges E. Analysis of plasmon resonance and surface-enhanced Raman scattering on periodic silver structures. Phys Rev B. 2000;61(20):14078.
10. Moskovits M, DiLella D, Maynard K. Surface Raman spectroscopy of a number of cyclic aromatic molecules adsorbed on silver: selection rules and molecular reorientation. Langmuir. 1988;4(1):67–76.
11. Moskovits M. Surface-enhanced spectroscopy. Rev Mod Phys. 1985;57(3):783.
12. Moskovits M. Surface-enhanced Raman spectroscopy: a brief retrospective. J Raman Spectrosc. 2005;36(6–7):485–96.
13. Schatz GC. Theoretical studies of surface enhanced Raman scattering. Acc Chem Res. 1984;17(10):370–6.
14. Schatz G, Young M, Van Duyne R. Electromagnetic mechanism of SERS. Surface-enhanced Raman scattering. Berlin: Springer; 2006. p. 19–45.
15. Nie S, Emory SR. Probing single molecules and single nanoparticles by surface-enhanced Raman scattering. Science. 1997;275(5303):1102–6.
16. Hatab NA, Hsueh C-H, Gaddis AL, Retterer ST, Li J-H, Eres G, et al. Free-standing optical gold bowtie nanoantenna with variable gap size for enhanced Raman spectroscopy. Nano Lett. 2010;10(12):4952–5.
17. Li S, Pedano ML, Chang S-H, Mirkin CA, Schatz GC. Gap structure effects on surface-enhanced Raman scattering intensities for gold gapped rods. Nano Lett. 2010;10(5):1722–7.
18. Lee SJ, Morrill AR, Moskovits M. Hot spots in silver nanowire bundles for surface-enhanced Raman spectroscopy. J Am Chem Soc. 2006;128(7):2200–1.
19. Jiang J, Bosnick K, Maillard M, Brus L. Single molecule Raman spectroscopy at the junctions of large Ag nanocrystals. Hamilton: ACS Publications; 2003.
20. Wang Y, Irudayaraj J. Surface-enhanced Raman spectroscopy at single-molecule scale and its implications in biology. Phil Trans R Soc B. 2013;368(1611):20120026.
21. Schlücker S. SERS microscopy: nanoparticle probes and biomedical applications. ChemPhysChem. 2009;10(9–10):1344–54.
22. Wang Y, Schlucker S. Rational design and synthesis of SERS labels. Analyst. 2013;138(8):2224–38.
23. Stern E, Vacic A, Rajan NK, Criscione JM, Park J, Ilic BR, et al. Label-free biomarker detection from whole blood. Nat Nanotechnol. 2010;5(2):138–42.
24. Laxman B, Morris DS, Yu J, Siddiqui J, Cao J, Mehra R, et al. A First-generation multiplex biomarker analysis of urine for the early detection of prostate cancer. Cancer Res. 2008;68(3):645–9.
25. Zhang A, Sun H, Wang X. Saliva metabolomics opens door to biomarker discovery, disease diagnosis, and treatment. Appl Biochem Biotechnol. 2012;168(6):1718–27.
26. Lane LA, Qian X, Nie S. SERS nanoparticles in medicine: from label-free detection to spectroscopic tagging. Chem Rev. 2015;115(19):10489–529.
27. Chan ECY, Koh PK, Mal M, Cheah PY, Eu KW, Backshall A, et al. Metabolic profiling of human colorectal cancer using high-resolution magic angle spinning nuclear magnetic resonance (HR-MAS NMR) spectroscopy and gas chromatography mass spectrometry (GC/MS). J Proteome Res. 2008;8(1):352–61.
28. Jia C-P, Zhong X-Q, Hua B, Liu M-Y, Jing F-X, Lou X-H, et al. Nano-ELISA for highly sensitive protein detection. Biosens Bioelectron. 2009;24(9):2836–41.
29. Vendrell M, Maiti KK, Dhaliwal K, Chang YT. Surface-enhanced Raman scattering in cancer detection and imaging. Trends Biotechnol. 2013;31(4):249–57.
30. Li Y, Wang Z, Mu X, Ma A, Guo S. Raman tags: novel optical probes for intracellular sensing and imaging. Biotechnol Adv. 2017;35(2):168–77.
31. Fabris L. Gold-based SERS tags for biomedical imaging. J Opt. 2015;17(11):114002.
32. Zhang Y, Hong H, Myklejord DV, Cai W. Molecular imaging with SERS-active nanoparticles. Small. 2011;7(23):3261–9.
33. Fabris L. SERS tags: the next promising tool for personalized cancer detection? Chem Nano Mat. 2016;2(4):249–58.
34. Sharma B, Frontiera RR, Henry A-I, Ringe E, Van Duyne RP. SERS: materials, applications, and the future. Mater Today. 2012;15(1):16–25.
35. Kneipp J, Kneipp H, Wittig B, Kneipp K. Novel optical nanosensors for probing and imaging live cells. Nanomed Nanotechnol Biol Med. 2010;6(2):214–26.
36. Seney CS, Gutzman BM, Goddard RH. Correlation of size and surface-enhanced Raman scattering activity of optical and spectroscopic properties for silver nanoparticles. J Phys Chem C. 2008;113(1):74–80.
37. Khlebtsov N, Dykman L. Biodistribution and toxicity of engineered gold nanoparticles: a review of in vitro and in vivo studies. Chem Soc Rev. 2011;40(3):1647–71.
38. Jain PK, Huang X, El-Sayed IH, El-Sayed MA. Review of some interesting surface plasmon resonance-enhanced properties of noble metal nanoparticles and their applications to biosystems. Plasmonics. 2007;2(3):107–18.
39. Van Duyne R, Hulteen J, Treichel D. Atomic force microscopy and surface-enhanced Raman spectroscopy. I. Ag island films and Ag film over polymer nanosphere surfaces supported on glass. J Chem Phys. 1993;99(3):2101–15.
40. Qiu C, Zhou H, Yang H, Chen M, Guo Y, Sun L. Investigation of n-layer graphenes as substrates for Raman enhancement of crystal violet. J Phys Chem C. 2011;115(20):10019–25.
41. Yang L, Gong M, Jiang X, Yin D, Qin X, Zhao B, et al. Investigation on SERS of different phase structure TiO_2 nanoparticles. J Raman Spectrosc. 2015;46(3):287–92.
42. Livingstone R, Zhou X, Tamargo MC, Lombardi JR, Quagliano LG, Jean-Mary F. Surface enhanced Raman spectroscopy of pyridine on CdSe/ZnBeSe quantum dots grown by molecular beam epitaxy. J Phys Chem C. 2010;114(41):17460–4.

43. Vo-Dinh T, Liu Y, Fales AM, Ngo H, Wang HN, Register JK, et al. SERS nanosensors and nanoreporters: golden opportunities in biomedical applications. Wiley interdiscip Rev Nanomed Nanobiotechnol. 2015;7(1):17–33.
44. Li W, Zamani R, Rivera Gil P, Pelaz B, Ibáñez M, Cadavid D, et al. CuTe nanocrystals: shape and size control, plasmonic properties, and use as SERS probes and photothermal agents. J Am Chem Soc. 2013;135(19):7098–101.
45. Guo P, Sikdar D, Huang X, Si KJ, Xiong W, Gong S, et al. Plasmonic core–shell nanoparticles for SERS detection of the pesticide thiram: size-and shape-dependent Raman enhancement. Nanoscale. 2015;7(7):2862–8.
46. Benz F, Chikkaraddy R, Salmon A, Ohadi H, de Nijs B, Mertens J, et al. SERS of individual nanoparticles on a mirror: size does matter, but so does shape. J Phys Chem Lett. 2016;7(12):2264–9.
47. Lu G, Forbes TZ, Haes AJ. SERS detection of uranyl using functionalized gold nanostars promoted by nanoparticle shape and size. Analyst. 2016;141(17):5137–43.
48. Brazhe N, Parshina E, Khabatova V, Semenova A, Brazhe A, Yusipovich A, et al. Tuning SERS for living erythrocytes: focus on nanoparticle size and plasmon resonance position. J Raman Spectrosc. 2013;44(5):686–94.
49. Mir-Simon B, Morla-Folch J, Gisbert-Quilis P, Pazos-Perez N, H-n Xie, Bastús NG, et al. SERS efficiencies of micrometric polystyrene beads coated with gold and silver nanoparticles: the effect of nanoparticle size. J Opt. 2015;17(11):114012.
50. Hu C, Shen J, Yan J, Zhong J, Qin W, Liu R, et al. Highly narrow nanogap-containing Au@ Au core–shell SERS nanoparticles: size-dependent Raman enhancement and applications in cancer cell imaging. Nanoscale. 2016;8(4):2090–6.
51. Lin K-Q, Yi J, Hu S, Liu B-J, Liu J-Y, Wang X, et al. Size effect on SERS of gold nanorods demonstrated via single nanoparticle spectroscopy. J Phys Chem C. 2016;120(37):20806–13.
52. Zheng P, Li M, Jurevic R, Cushing SK, Liu Y, Wu N. A gold nanohole array based surface-enhanced Raman scattering biosensor for detection of silver (I) and mercury (II) in human saliva. Nanoscale. 2015;7(25):11005–12.
53. Yue W, Yang Y, Wang Z, Han J, Syed A, Chen L, et al. Improved surface-enhanced Raman scattering on arrays of gold quasi-3D nanoholes. J Phys D Appl Phys. 2012;45(42):425401.
54. Kahraman M, Wachsmann-Hogiu S. Label-free and direct protein detection on 3D plasmonic nanovoid structures using surface-enhanced Raman scattering. Anal Chim Acta. 2015;856:74–81.
55. Driskell JD, Kwarta KM, Lipert RJ, Porter MD, Neill JD, Ridpath JF. Low-level detection of viral pathogens by a surface-enhanced Raman scattering based immunoassay. Anal Chem. 2005;77(19):6147–54.
56. Daniel M-C, Astruc D. Gold nanoparticles: assembly, supramolecular chemistry, quantum-size-related properties, and applications toward biology, catalysis, and nanotechnology. Chem Rev. 2004;104(1):293–346.
57. Liu S, Zheng X, Song L, Liu W, Yao T, Sun Z, et al. Partial-surface-passivation strategy for transition-metal-based copper–gold nanocage. Chem Commun. 2016;52(39):6617–20.
58. Wang M, Cao X, Lu W, Tao L, Zhao H, Wang Y, et al. Surface-enhanced Raman scattering immunoassay for carcinoembryonic antigen based on gold nanostars. J Nanosci Nanotechnol. 2016;16(7):6711–8.
59. Zhang Q, Moran CH, Xia X, Rycenga M, Li N, Xia Y. Synthesis of Ag nanobars in the presence of single-crystal seeds and a bromide compound, and their surface-enhanced Raman scattering (SERS) properties. Langmuir. 2012;28(24):9047–54.
60. Wei H, Reyes-Coronado A, Nordlander P, Aizpurua J, Xu H. Multipolar plasmon resonances in individual Ag nanorice. ACS Nano. 2010;4(5):2649–54.
61. Boca SC, Farcau C, Astilean S. The study of Raman enhancement efficiency as function of nanoparticle size and shape. Nucl Instrum Methods Phys Res, Sect B. 2009;267(2):406–10.
62. Yoon JK, Kim K, Shin KS. Raman scattering of 4-aminobenzenethiol sandwiched between Au nanoparticles and a macroscopically smooth Au substrate: effect of size of Au nanoparticles. J Phys Chem C. 2009;113(5):1769–74.
63. Kahraman M, Mullen ER, Korkmaz A, Wachsmann-Hogiu S. Fundamentals and applications of SERS-based bioanalytical sensing. Nanophotonics. 2017;6(5):831–52.
64. Cinel NA, Bütün S, Ertaş G, Özbay E. 'Fairy Chimney'-shaped tandem metamaterials as double resonance SERS substrates. Small. 2013;9(4):531–7.
65. Laing S, Jamieson LE, Faulds K, Graham D. Surface-enhanced Raman spectroscopy for in vivo biosensing. Nature Reviews Chemistry. 2017;1(8):0060.
66. Küstner B, Gellner M, Schütz M, Schöppler F, Marx A, Ströbel P, et al. SERS labels for red laser excitation: silica-encapsulated SAMs on tunable gold/silver nanoshells. Angew Chem Int Ed. 2009;48(11):1950–3.
67. Graham D, Faulds K, Smith WE. Biosensing using silver nanoparticles and surface enhanced resonance Raman scattering. Chem Commun. 2006;42:4363–71.
68. Graham D, Smith WE, Linacre AM, Munro CH, Watson ND, White PC. Selective detection of deoxyribonucleic acid at ultralow concentrations by SERRS. Anal Chem. 1997;69(22):4703–7.
69. Graham D, Mallinder BJ, Smith WE. Surface-enhanced resonance Raman scattering as a novel Method of DNA discrimination. Angew Chem. 2000;112(6):1103–5.
70. Faulds K, McKenzie F, Smith WE, Graham D. Quantitative simultaneous multianalyte detection of DNA by dual-wavelength surface-enhanced resonance Raman scattering. Angew Chem. 2007;119(11):1861–3.
71. Indrasekara A, Paladini BJ, Naczynski DJ, Starovoytov V, Moghe PV, Fabris L. Dimeric Gold Nanoparticle Assemblies as Tags for SERS-Based Cancer Detection. Advanced healthcare materials. 2013;2(10):1370–6.
72. Mulvaney SP, Musick MD, Keating CD, Natan MJ. Glass-coated, analyte-tagged nanoparticles: a new tagging system based on detection with surface-enhanced Raman scattering. Langmuir. 2003;19(11):4784–90.
73. Doering WE, Nie S. Spectroscopic tags using dye-embedded nanoparticles and surface-enhanced Raman scattering. Anal Chem. 2003;75(22):6171–6.
74. Tripp RA, Dluhy RA, Zhao Y. Novel nanostructures for SERS biosensing. Nano Today. 2008;3(3):31–7.
75. Qian XM, Nie SM. Single-molecule and single-nanoparticle SERS: from fundamental mechanisms to biomedical applications. Chem Soc Rev. 2008;37(5):912–20.
76. Li W, Camargo PH, Lu X, Xia Y. Dimers of silver nanospheres: facile synthesis and their use as hot spots for surface-enhanced Raman scattering. Nano Lett. 2009;9(1):485–90.
77. Lim DK, Jeon KS, Hwang JH, Kim H, Kwon S, Suh YD, et al. Highly uniform and reproducible surface-enhanced Raman scattering from DNA-tailorable nanoparticles with 1-nm interior gap. Nat Nanotechnol. 2011;6(7):452–60.
78. Liu R, Liu B, Guan G, Jiang C, Zhang Z. Multilayered shell SERS nanotags with a highly uniform single-particle Raman readout for ultrasensitive immunoassays. Chem Commun. 2012;48(75):9421–3.
79. Cao J, Zhao D, Mao Q. A highly reproducible and sensitive fiber SERS probe fabricated by direct synthesis of closely packed AgNPs on the silanized fiber taper. Analyst. 2017;142(4):596–602.

80. Zheng X-S, Hu P, Cui Y, Zong C, Feng J-M, Wang X, et al. BSA-coated nanoparticles for improved SERS-based intracellular pH sensing. Anal Chem. 2014;86(24):12250–7.
81. Gühlke M, Heiner Z, Kneipp J. Combined near-infrared excited SEHRS and SERS spectra of pH sensors using silver nanostructures. Phys Chem Chem Phys. 2015;17(39):26093–100.
82. Wang F, Widejko RG, Yang Z, Nguyen KT, Chen H, Fernando LP, et al. Surface-enhanced Raman scattering detection of pH with silica-encapsulated 4-mercaptobenzoic acid-functionalized silver nanoparticles. Anal Chem. 2012;84(18):8013–9.
83. Jamieson LE, Jaworska A, Jiang J, Baranska M, Harrison D, Campbell C. Simultaneous intracellular redox potential and pH measurements in live cells using SERS nanosensors. Analyst. 2015;140(7):2330–5.
84. Liu Y, Yuan H, Fales AM, Vo-Dinh T. pH-sensing nanostar probe using surface-enhanced Raman scattering (SERS): theoretical and experimental studies. J Raman Spectrosc. 2013;44(7):980–6.
85. Chen P, Wang Z, Zong S, Chen H, Zhu D, Zhong Y, et al. A wide range optical pH sensor for living cells using Au@ Ag nanoparticles functionalized carbon nanotubes based on SERS signals. Anal Bioanal Chem. 2014;406(25):6337–46.
86. Kneipp J, Kneipp H, Wittig B, Kneipp K. One- and two-photon excited optical ph probing for cells using surface-enhanced Raman and hyper-Raman nanosensors. Nano Lett. 2007;7(9):2819–23.
87. Kneipp J, Kneipp H, Wittig B, Kneipp K. Following the dynamics of pH in endosomes of live cells with SERS nanosensors. J Phys Chem C. 2010;114(16):7421–6.
88. Talley CE, Jusinski L, Hollars CW, Lane SM, Huser T. Intracellular pH sensors based on surface-enhanced Raman scattering. Anal Chem. 2004;76(23):7064–8.
89. Kong KV, Dinish U, Lau WKO, Olivo M. Sensitive SERS-pH sensing in biological media using metal carbonyl functionalized planar substrates. Biosens Bioelectron. 2014;54:135–40.
90. Pang Y, Wang J, Xiao R, Wang S. SERS molecular sentinel for the RNA genetic marker of PB1-F2 protein in highly pathogenic avian influenza (HPAI) virus. Biosens Bioelectron. 2014;61:460–5.
91. Gu X, Yan Y, Jiang G, Adkins J, Shi J, Jiang G, et al. Using a silver-enhanced microarray sandwich structure to improve SERS sensitivity for protein detection. Anal Bioanal Chem. 2014;406(7):1885–94.
92. Zhou L, Ding F, Chen H, Ding W, Zhang W, Chou SY. Enhancement of immunoassay's fluorescence and detection sensitivity using three-dimensional plasmonic nano-antenna-dots array. Anal Chem. 2012;84(10):4489–95.
93. Lv Y, Qin Y, Svec F, Tan T. Molecularly imprinted plasmonic nanosensor for selective SERS detection of protein biomarkers. Biosens Bioelectron. 2016;80:433–41.
94. Shin MH, Hong W, Sa Y, Chen L, Jung Y-J, Wang X, et al. Multiple detection of proteins by SERS-based immunoassay with core shell magnetic gold nanoparticles. Vib Spectrosc. 2014;72:44–9.
95. Wang Y, Vaidyanathan R, Shiddiky MJ, Trau M. Enabling rapid and specific surface-enhanced Raman scattering immunoassay using nanoscaled surface shear forces. ACS Nano. 2015;9(6):6354–62.
96. Kamil Reza K, Wang J, Vaidyanathan R, Dey S, Wang Y, Trau M. Electrohydrodynamic-induced SERS immunoassay for extensive multiplexed biomarker sensing. Small. 2017;13(9):1602902.
97. Wang Y, Lee K, Irudayaraj J. SERS aptasensor from nanorod-nanoparticle junction for protein detection. Chem Commun. 2010;46(4):613–5.
98. Wang Y, Rauf S, Grewal YS, Spadafora LJ, Shiddiky MJ, Cangelosi GA, et al. Duplex microfluidic SERS detection of pathogen antigens with nanoyeast single-chain variable fragments. Anal Chem. 2014;86(19):9930–8.
99. Cheng Z, Choi N, Wang R, Lee S, Moon KC, Yoon SY, et al. Simultaneous detection of dual prostate specific antigens using surface-enhanced Raman scattering-based immunoassay for accurate diagnosis of prostate cancer. ACS Nano. 2017;11(5):4926–33.
100. Ngo HT, Wang H-N, Fales AM, Vo-Dinh T. Label-free DNA biosensor based on SERS molecular sentinel on nanowave chip. Anal Chem. 2013;85(13):6378–83.
101. Qi J, Zeng J, Zhao F, Lin SH, Raja B, Strych U, et al. Label-free, in situ SERS monitoring of individual DNA hybridization in microfluidics. Nanoscale. 2014;6(15):8521–6.
102. Bi L, Rao Y, Tao Q, Dong J, Su T, Liu F, et al. Fabrication of large-scale gold nanoplate films as highly active SERS substrates for label-free DNA detection. Biosens Bioelectron. 2013;43:193–9.
103. Liu M, Wang Z, Zong S, Zhang R, Zhu D, Xu S, et al. SERS-based DNA detection in aqueous solutions using oligonucleotide-modified Ag nanoprisms and gold nanoparticles. Anal Bioanal Chem. 2013;405(18):6131–6.
104. Chen Y, Chen G, Zheng X, He C, Feng S, Chen Y, et al. Discrimination of gastric cancer from normal by serum RNA based on surface-enhanced Raman spectroscopy (SERS) and multivariate analysis. Med Phys. 2012;39(9):5664–8.
105. Guven B, Dudak FC, Boyaci IH, Tamer U, Ozsoz M. SERS-based direct and sandwich assay methods for mir-21 detection. Analyst. 2014;139(5):1141–7.
106. Wang X, Choi N, Cheng Z, Ko J, Chen L, Choo J. Simultaneous detection of dual nucleic acids using a SERS-based lateral flow assay biosensor. Anal Chem. 2017;89(2):1163–9.
107. Wang Y, Wee EJ, Trau M. Highly sensitive DNA methylation analysis at CpG resolution by surface-enhanced Raman scattering via ligase chain reaction. Chem Commun. 2015;51(54):10953–6.
108. Wee EJ, Wang Y, Tsao SC, Trau M. Simple, sensitive and accurate multiplex detection of clinically important melanoma dna mutations in circulating tumour DNA with SERS nanotags. Theranostics. 2016;6(10):1506–13.
109. Koo KM, Wee EJ, Mainwaring PN, Wang Y, Trau M. Toward precision medicine: a cancer molecular subtyping Nanostrategy for RNA biomarkers in tumor and urine. Small. 2016;12(45):6233–42.
110. Gupta VK, Atar N, Yola ML, Eryılmaz M, Torul H, Tamer U, et al. A novel glucose biosensor platform based on Ag@ AuNPs modified graphene oxide nanocomposite and SERS application. J Coll Interface Sci. 2013;406:231–7.
111. Shafer-Peltier KE, Haynes CL, Glucksberg MR, Van Duyne RP. Toward a glucose biosensor based on surface-enhanced Raman scattering. J Am Chem Soc. 2003;125(2):588–93.
112. Kong KV, Lam Z, Lau WKO, Leong WK, Olivo M. A transition metal carbonyl probe for use in a highly specific and sensitive SERS-based assay for glucose. J Am Chem Soc. 2013;135(48):18028–31.
113. Ding X, Kong L, Wang J, Fang F, Li D, Liu J. Highly sensitive SERS detection of Hg^{2+} ions in aqueous media using gold nanoparticles/graphene heterojunctions. ACS Appl Mater Interfaces. 2013;5(15):7072–8.
114. Crane LG, Wang D, Sears LM, Heyns B, Carron K. SERS surfaces modified with a 4-(2-pyridylazo) resorcinol disulfide derivative: detection of copper, lead, and cadmium. Anal Chem. 1995;67(2):360–4.
115. Wang Y, Irudayaraj J. A SERS DNAzyme biosensor for lead ion detection. Chem Commun. 2011;47(15):4394–6.
116. Li F, Wang J, Lai Y, Wu C, Sun S, He Y, et al. Ultrasensitive and selective detection of copper (II) and mercury (II) ions by dye-coded silver nanoparticle-based SERS probes. Biosens Bioelectron. 2013;39(1):82–7.

117. Žukovskaja O, Jahn IJ, Weber K, Cialla-May D, Popp J. Detection of Pseudomonas aeruginosa Metabolite Pyocyanin in Water and Saliva by Employing the SERS Technique. Sensors. 2017;17(8):1704.
118. Choi CJ, Wu H-Y, George S, Weyhenmeyer J, Cunningham BT. Biochemical sensor tubing for point-of-care monitoring of intravenous drugs and metabolites. Lab Chip. 2012;12(3):574–81.
119. Yang T, Guo X, Wang H, Fu S, Yang H. Magnetically optimized SERS assay for rapid detection of trace drug-related biomarkers in saliva and fingerprints. Biosens Bioelectron. 2015;68:350–7.
120. Šimáková P, Kočišová E, Procházka M. Sensitive Raman spectroscopy of lipids based on drop deposition using DCDR and SERS. J Raman Spectrosc. 2013;44(11):1479–82.
121. Levin CS, Kundu J, Janesko BG, Scuseria GE, Raphael RM, Halas NJ. Interactions of ibuprofen with hybrid lipid bilayers probed by complementary surface-enhanced vibrational spectroscopies. J Physical Chemistry B. 2008;112(45):14168–75.
122. Xie Y, Xu L, Wang Y, Shao J, Wang L, Wang H, et al. Label-free detection of the foodborne pathogens of Enterobacteriaceae by surface-enhanced Raman spectroscopy. Anal Methods. 2013;5(4):946–52.
123. Wang Y, Ravindranath S, Irudayaraj J. Separation and detection of multiple pathogens in a food matrix by magnetic SERS nanoprobes. Anal Bioanal Chem. 2011;399(3):1271–8.
124. Tannock IF, Rotin D. Acid pH in tumors and its potential for therapeutic exploitation. Cancer Res. 1989;49(16):4373–84.
125. Hashim AI, Zhang X, Wojtkowiak JW, Martinez GV, Gillies RJ. Imaging pH and metastasis. NMR Biomed. 2011;24(6):582–91.
126. Porter MD, Lipert RJ, Siperko LM, Wang G, Narayanan R. SERS as a bioassay platform: fundamentals, design, and applications. Chem Soc Rev. 2008;37(5):1001–11.
127. Bantz KC, Meyer AF, Wittenberg NJ, Im H, Kurtuluş Ö, Lee SH, et al. Recent progress in SERS biosensing. Phys Chem Chem Phys. 2011;13(24):11551–67.
128. Mead PS, Slutsker L, Dietz V, McCaig LF, Bresee JS, Shapiro C, et al. Food-related illness and death in the United States. Emerg Infect Dis. 1999;5(5):607–25.
129. Schütz M, Steinigeweg D, Salehi M, Kömpe K, Schlücker S. Hydrophilically stabilized gold nanostars as SERS labels for tissue imaging of the tumor suppressor p63 by immuno-SERS microscopy. Chem Commun. 2011;47(14):4216–8.
130. Salehi M, Steinigeweg D, Ströbel P, Marx A, Packeisen J, Schlücker S. Rapid immuno-SERS microscopy for tissue imaging with single-nanoparticle sensitivity. J Biophoton. 2013;6(10):785–92.
131. Potara M, Bawaskar M, Simon T, Gaikwad S, Licarete E, Ingle A, et al. Biosynthesized silver nanoparticles performing as biogenic SERS-nanotags for investigation of C26 colon carcinoma cells. Coll Surf B. 2015;133:296–303.
132. Dinish US, Balasundaram G, Chang Y-T, Olivo M. Actively targeted in vivo multiplex detection of intrinsic cancer biomarkers using biocompatible SERS nanotags. Sci Rep. 2014;4:4075.
133. Yuan H, Liu Y, Fales AM, Li YL, Liu J, Vo-Dinh T. Quantitative surface-enhanced resonant Raman scattering multiplexing of biocompatible gold nanostars for in vitro and ex vivo detection. Anal Chem. 2012;85(1):208–12.
134. Xiao M, Lin L, Li Z, Liu J, Hong S, Li Y, et al. SERS imaging of cell-surface biomolecules metabolically labeled with bioorthogonal Raman reporters. Chem Asian J. 2014;9(8):2040–4.
135. Zhang Y, Qian J, Wang D, Wang Y, He S. Multifunctional gold nanorods with ultrahigh stability and tunability for in vivo fluorescence imaging, SERS detection, and photodynamic therapy. Angewandte Chemie Int Ed. 2013;52(4):1148–51.
136. McVeigh PZ, Mallia RJ, Veilleux I, Wilson BC. Widefield quantitative multiplex surface enhanced Raman scattering imaging in vivo. J Biomed Opt. 2013;18(4):046011.
137. Niu X, Chen H, Wang Y, Wang W, Sun X, Chen L. Upconversion fluorescence-SERS dual-mode tags for cellular and in vivo imaging. ACS Appl Mater Interfaces. 2014;6(7):5152–60.
138. Liu Y, Ashton JR, Moding EJ, Yuan H, Register JK, Fales AM, et al. A plasmonic gold nanostar theranostic probe for in vivo tumor imaging and photothermal therapy. Theranostics. 2015;5(9):946–60.
139. Mallia RJ, McVeigh PZ, Veilleux I, Wilson BC. Filter-based method for background removal in high-sensitivity wide-field-surface-enhanced Raman scattering imaging in vivo. J Biomed Opt. 2012;17(7):0760171–5.
140. Wang Y, Seebald JL, Szeto DP, Irudayaraj J. Biocompatibility and biodistribution of surface-enhanced Raman scattering nanoprobes in zebrafish embryos: in vivo and multiplex imaging. ACS Nano. 2010;4(7):4039–53.
141. Yigit MV, Zhu L, Ifediba MA, Zhang Y, Carr K, Moore A, et al. Noninvasive MRI-SERS imaging in living mice using an innately bimodal nanomaterial. ACS Nano. 2010;5(2):1056–66.
142. Yigit MV, Medarova Z. In vivo and ex vivo applications of gold nanoparticles for biomedical SERS imagingi. Am J Nucl Med Mol Imaging. 2012;2(2):232–41.
143. Jokerst JV, Miao Z, Zavaleta C, Cheng Z, Gambhir SS. Affibody-functionalized gold-silica nanoparticles for Raman molecular imaging of the epidermal growth factor receptor. Small. 2011;7(5):625–33.
144. Chen Y, Zheng X, Chen G, He C, Zhu W, Feng S, et al. Immunoassay for LMP1 in nasopharyngeal tissue based on surface-enhanced Raman scattering. Int J Nanomed. 2012;7:73–82.
145. Schlücker S, Küstner B, Punge A, Bonfig R, Marx A, Ströbel P. Immuno-Raman microspectroscopy: in situ detection of antigens in tissue specimens by surface-enhanced Raman scattering. J Raman Spectrosc. 2006;37(7):719–21.
146. Lee S, Chon H, Lee J, Ko J, Chung BH, Lim DW, et al. Rapid and sensitive phenotypic marker detection on breast cancer cells using surface-enhanced Raman scattering (SERS) imaging. Biosens Bioelectron. 2014;51:238–43.
147. Nima ZA, Mahmood M, Xu Y, Mustafa T, Watanabe F, Nedosekin DA, et al. Circulating tumor cell identification by functionalized silver-gold nanorods with multicolor, super-enhanced SERS and photothermal resonances. Sci Rep. 2014;4:4752.
148. Liu R, Zhao J, Han G, Zhao T, Zhang R, Liu B, et al. Click-functionalized SERS nanoprobes with improved labeling efficiency and capability for cancer cell imaging. ACS Appl Mater Interfaces. 2017;9(44):38222–9.
149. Oseledchyk A, Andreou C, Wall MA, Kircher MF. Folate-targeted surface-enhanced resonance Raman scattering nanoprobe ratiometry for detection of microscopic ovarian cancer. ACS Nano. 2017;11(2):1488–97.